THE JOURNAL OF BIOLOGICAL CHEMISTRY VOL. 288, NO. 29, pp. 21458–21472, July 19, 2013

Altered Cortical $GABA_A$ Receptor Composition, Physiology, and Endocytosis in a Mouse Model of a Human Genetic Absence Epilepsy Syndrome*

Received for publication, December 13, 2012, and in revised form, May 26, 2013 Published, JBC Papers in Press, June 6, 2013, DOI 10.1074/jbc.M112.444372

Chengwen Zhou, Zhiling Huang,[1] Li Ding, M. Elizabeth Deel, Fazal M. Arain, Clark R. Murray, Ronak S. Patel, Christopher D. Flanagan, and Martin J. Gallagher[2]

From the Department of Neurology, Vanderbilt University, Nashville, Tennessee 37232

Background: Heterozygous GABRA1 deletion causes absence epilepsy.
Results: The deletion modestly decreased cortical $GABA_A$ receptor number but also reduced the rate of receptor endocytosis and thus partially compensated for the deletion by increasing the expression of different receptor isoforms.
Conclusion: Heterozygous GABRA1 deletion caused novel alterations in cortical $GABA_A$ receptor expression and physiology.
Significance: These findings reveal mechanisms of cortical disinhibition in absence epilepsy.

Patients with generalized epilepsy exhibit cerebral cortical disinhibition. Likewise, mutations in the inhibitory ligand-gated ion channels, $GABA_A$ receptors ($GABA_A$Rs), cause generalized epilepsy syndromes in humans. Recently, we demonstrated that heterozygous knock-out ($Het_{\alpha 1}KO$) of the human epilepsy gene, the $GABA_A$R α1 subunit, produced absence epilepsy in mice. Here, we determined the effects of $Het_{\alpha 1}KO$ on the expression and physiology of $GABA_A$Rs in the mouse cortex. We found that $Het_{\alpha 1}KO$ caused modest reductions in the total and surface expression of the β2 subunit but did not alter β1 or β3 subunit expression, results consistent with a small reduction of $GABA_A$Rs. Cortices partially compensated for $Het_{\alpha 1}KO$ by increasing the fraction of residual α1 subunit on the cell surface and by increasing total and surface expression of α3, but not α2, subunits. Co-immunoprecipitation experiments revealed that $Het_{\alpha 1}KO$ increased the fraction of α1 subunits, and decreased the fraction of α3 subunits, that associated in hybrid $\alpha 1\alpha 3\beta\gamma$ receptors. Patch clamp electrophysiology studies showed that $Het_{\alpha 1}KO$ layer VI cortical neurons exhibited reduced inhibitory postsynaptic current peak amplitudes, prolonged current rise and decay times, and altered responses to benzodiazepine agonists. Finally, application of inhibitors of dynamin-mediated endocytosis revealed that $Het_{\alpha 1}KO$ reduced base-line $GABA_A$R endocytosis, an effect that probably contributes to the observed changes in $GABA_A$R expression. These findings demonstrate that $Het_{\alpha 1}KO$ exerts two principle disinhibitory effects on cortical $GABA_A$R-mediated inhibitory neurotransmission: 1) a modest reduction of $GABA_A$R number and 2) a partial compensation with $GABA_A$R isoforms that possess physiological properties different from those of the otherwise predominant $\alpha 1\beta\gamma$ $GABA_A$Rs.

Under normal physiological conditions, cortical excitatory and inhibitory activity exists in a coordinated homeostasis (1, 2). However, studies of humans and rodents with generalized epilepsy, syndromes in which the seizure activity originates from both cerebral hemispheres at the time of onset, suggest that cortical disinhibition contributes to the pathophysiology of these diseases (3–5). Therefore, it is critical to understand the biochemical mechanisms that alter cortical inhibitory networks in generalized epilepsy syndromes in order to identify new treatments for these diseases.

$GABA_A$ receptors ($GABA_A$Rs)[3] are the predominant inhibitory ligand-gated ion channels in the mammalian brain. They are pentamers whose five subunits originate from eight gene families that contain multiple isoforms (α1–6, β1–3, γ1–3, δ, ϵ, θ, π, and ρ1–3). These 19 subunits can combine in many different ways to form functional receptors, but most synaptic receptors in the cortex contain two α subunits (α1–3 isoforms), two β subunits, and a γ subunit arranged in the order γ-β-α-β-α (6). The identity of the α subunit isoform that is incorporated into the $GABA_A$R affects the physiological properties. For example, $\alpha 3\beta\gamma$ receptors have lower GABA sensitivity and prolonged current activation and deactivation times than $\alpha 1\beta\gamma$ or $\alpha 2\beta\gamma$ receptors (7).

Four autosomal dominant mutations (A322D, S326fs328X, D219N, and K353delins18X) in the $GABA_A$R α1 subunit associate with generalized epilepsy (8–10). *In vitro* studies demonstrated that each of these mutations results in a substantial loss of α1 subunit function or expression (9, 11, 12). In particular, the S326fs328X mutation, which causes absence epilepsy, caused complete elimination of mutant α1 subunit protein (12). Therefore, it was thought that S326fs328X conferred absence epilepsy by producing a heterozygous loss of α1 subunit expression. This hypothesis was supported by our recent observation

* This work was supported, in whole or in part, by National Institutes of Health Grants R01 NS064286 and K02 NS055979 (to M. J. G.).
[1] Present address: Department of Neurology, The Second Xiangya Hospital, Central South University, Changsha, Hunan 410011, China.
[2] To whom correspondence should be addressed: Dept. of Neurology, Vanderbilt University, 6114 Medical Research Bldg. III, 465 21st Ave. S., Nashville, TN 37232-8552. Tel.: 615-322-5979; Fax: 615-322-5517; E-mail: Martin.Gallagher@Vanderbilt.edu.

[3] The abbreviations used are: $GABA_A$R, $GABA_A$ receptor; aCSF, artificial cerebrospinal fluid; RIPA, radioimmunoprecipitation assay; ER, endoplasmic reticulum; endo-H, endoglycosidase H; PNGase F, peptide:*N*-glycosidase F; IPSC, inhibitory postsynaptic current; mIPSC, miniature IPSC; eIPSC, evoked IPSC; K-S, Kolmogorov-Smirnov.

that heterozygous α1 subunit knock-out (Het$_{\alpha1}$KO) mice exhibited absence epilepsy (13).

Previous studies designed to investigate the developmental role of the α1 subunit in GABAergic neurotransmission demonstrated that neurons with a homozygous α1 subunit deletion increased the total expression of other α subunits that they normally expressed rather than expressing new α subunit isoforms (14–21). Here, we elucidated how the epilepsy-associated heterozygous α1 subunit deletion affects synaptic-type GABA$_A$R expression and physiology in the cortices of Het$_{\alpha1}$KO mice.

We quantified the effects of Het$_{\alpha1}$KO on both total and cell surface synaptic type GABA$_A$R expression because it is surface expression that affects GABA$_A$R physiology. We then determined the effects of Het$_{\alpha1}$KO on GABAergic synaptic physiology and pharmacology. Finally, we identified the effects of Het$_{\alpha1}$KO on constitutive GABA$_A$R endocytosis/recycling, a cellular mechanism that dynamically modulates GABA$_A$R surface expression. These experiments identified modifications in cortical GABA$_A$R surface expression, composition, physiology, and endocytosis that probably contribute to the pathophysiology of seizures in the Het$_{\alpha1}$KO model of absence epilepsy and, importantly, may also be involved in regulating GABA$_A$ receptor expression and physiology in other diseases that result from GABA$_A$ receptor dysfunction.

EXPERIMENTAL PROCEDURES

Animals—We performed all procedures using protocols approved by the Vanderbilt University Institutional Animal Care and Use Committee. The mice were housed in a controlled facility with a 12-h light/dark schedule, a temperature- and humidity-controlled environment, and *ad libitum* water and food. Vicini *et al.* (22) produced mice with loxP sequences surrounding exon 9 of the GABA$_A$R α1 subunit. We recently generated an unconditional α1 subunit deletion using these mice and bred them into a congenic C57BL/6J background (13). We mated wild type and Het$_{\alpha1}$KO mice and utilized female pups at postnatal ages 33–37 because our previous EEG studies identified frequent absence seizures in female Het$_{\alpha1}$KO mice at this age (13).

We also used homozygous α1 subunit deletion mice and male α3 subunit deletion mice (23) to verify specificity of the anti-α1 subunit and anti-α3 subunit antibodies in immunofluorescence experiments. Breeding pairs of α3 subunit deletion mice were a generous gift from Dr. Uwe Rudolph (Harvard Medical School). All mice were genotyped with PCR before experiments.

Cell Culture, Expression Vectors, and Transfection—COS-7 cells were cultured in 5% CO_2, 95% air at 37 °C in Dulbecco's modified Eagle's medium (Invitrogen) with 100 IU/ml penicillin and streptomycin and 10% fetal bovine serum (FBS; Invitrogen). We replated the cells twice weekly. A description of plasmids expressing the α1, α3, β2, and γ2 subunits was published previously (11). A plasmid expressing the β1 subunit was a generous gift from Dr. Robert Macdonald (Vanderbilt University). COS-7 cells were transfected with 3 μg of total DNA using FuGENE 6 transfection reagent (Roche Applied Science).

Brain Slice Preparation—Mice were anesthetized with isoflurane and sacrificed. Brains were rapidly dissected and placed for sectioning in cutting solution kept at 0 °C. For the brain slice biotinylation experiments, the cutting solution contained 210 mM sucrose, 20 mM NaCl, 2.5 mM KCl, 1.2 mM NaH_2PO_4, 1 mM $MgCl_2$, and 10 mM D-glucose, pH 7.4, bubbled with 100% O_2 at 0 °C. Three to four sagittal cortex slices (300 μm) were sectioned from the midline with a vibratome (Leica VT1200S). The slices were kept in artificial cerebrospinal fluid (aCSF), containing 126 mM NaCl, 2.5 mM KCl, 1.25 mM NaH_2PO_4, 2 mM $CaCl_2$, 1 mM $MgCl_2$, and 10 mM D-glucose, pH 7.4, bubbled with 100% O_2 at 0 °C until biotinylation, which occurred less than 1 h after the slices were made.

Brain slices for the electrophysiology experiments were made in 214 mM sucrose, 2.5 mM KCl, 1.25 mM NaH_2PO_4, 0.5 mM $CaCl_2$, 10 mM $MgSO_4$, 24 mM $NaHCO_3$, and 11 mM D-glucose, pH 7.4, bubbled with 95% O_2, 5% CO_2 at 4 °C. We made 300-μm coronal slices that contained the somatosensory cortex. Slices were then incubated in aCSF that contained 26 mM $NaHCO_3$ and 2 mM $MgCl_2$ and was bubbled with 95% O_2, 5% CO_2 at 36 °C for 30 min (24–26). The slices were then kept at room temperature for at least 1 h before electrophysiological recordings.

Antibodies and Western Blots—We obtained the antibodies from the following sources and listed the clone or catalogue number and the concentrations used for the Western blots in parentheses. The purified mouse monoclonal anti-GABA$_A$R α1 subunit (N95/35, 1:250), anti-β1 subunit (N96/55, 1:100), and anti-β3 subunit (N87/25, 1:100) antibodies were from the University of California Davis/National Institutes of Health NeuroMab Facility. The rabbit polyclonal anti GABA$_A$R β2 subunit antibody (AB5561, 1:100) was from Millipore, and the rabbit polyclonal anti-GABA$_A$R α2 subunit was from Abcam (AB72445, 1:100). The anti-α3 subunit antibody was from Alomone (AGA-003, 1:500). The mouse monoclonal anti-Na^+/K^+ ATPase α subunit (a6F, 1:100) was from the Developmental Studies Hybridoma Bank, and the rabbit polyclonal anti-glyceraldehyde-3-phosphate dehydrogenase (GAPDH) antibody (AB9485, 1:2000) was from Abcam. The fluorescently conjugated goat anti rabbit-680 (926-32221) and goat anti mouse-800 (926-32210) secondary antibodies were from LI-COR (1:10,000).

Total and surface proteins were fractionated on 10% SDS-polyacrylamide gels and then electrotransferred to nitrocellulose membranes. To ensure linearity of detection, 5, 10, and 15 μg of total protein and 5, 10, and 20 μl of protein eluted from either the neutravidin or protein G beads were applied to the gel; Western blots in which the signal from each protein did not increase in proportion to the amount loaded on the gel were excluded from analyses. Nonspecific binding was blocked with 5% nonfat dry milk in Tris-buffered saline containing 0.1% Tween, pH 7.4. We incubated the blots with primary antibody at 4 °C overnight and then with secondary antibody at room temperature for 1 h. The blots were imaged on an infrared fluorescent imaging system (LI-COR Biosciences).

Brain Slice Biotinylation—Using a brain slice biotinylation assay to quantify protein expressed on the cell surface in intact brain slices has been described previously (27–29). Briefly, after

cutting, the brain slices were incubated for 45 min at 4 °C in aCSF that contained 1 mg/ml of the membrane-impermeable, biotinylation reagent, sulfosuccinimidyl-2-(biotinamido)-ethyl-1,3′-dithiopropionate (Sulfo-NHS-SS-biotin; Thermo Scientific). After biotinylation, the slices were washed with 0.1 M glycine in aCSF. The cortices were dissected and sonicated in radioimmunoprecipitation assay (RIPA) solution (20 mM Tris, pH 7.4, 1% Triton X-100, 250 mM NaCl) that also contained protease inhibitor mixture (1:100; Sigma-Aldrich), 0.5% deoxycholate, and 0.1% SDS.

Protein concentrations were determined using a bicinchoninic acid-based assay (Thermo Scientific). To isolate the biotinylated surface protein, we incubated 150 μg of cortical protein lysate overnight at 4 °C with 100 μl of neutravidin beads (Thermo Scientific) in a final volume of 500 μl of RIPA buffer. In addition, in initial experiments, we confirmed that the neutravidin beads did not saturate with biotinylated protein by incubating the beads with larger masses of cortical protein lysate and observing proportional increases in the amounts of biotinylated material recovered from the beads. After incubation, the beads were pelleted by centrifugation and washed three times with RIPA buffer before the biotinylated protein was liberated using 60–80 μl of Laemmli sample buffer (Bio-Rad) containing 5% β-mercaptoethanol. The recovered protein was then analyzed by Western blot.

Immunofluorescence and Confocal Microscopy—Immunofluoresnce experiments were performed essentially as described previously (19). Briefly, we cut 2-mm coronal block slices (Zivic Instruments) of fresh brain tissue in the anterior parietal cortex and fixed them in 4% paraformaldehyde dissolved in 10 mM sodium phosphate buffer at 0 °C for 30 min. The brain slices were cryoprotected overnight in 30% sucrose in phosphate-buffered saline (PBS) at 4 °C and then sectioned (15 μm) on a cryostat (Leica) onto Shandon Colorfrost Plus glass slides (Thermo Scientific).

The slices were blocked (10% donkey serum, 2% Triton X-100 in PBS) for 1 h at room temperature. They were then incubated overnight at 4 °C with either rabbit anti-α1 subunit antibody (06868, 1:250; Millipore) or rabbit anti α3 subunit antibody (AGA-003, 1:500; Alomone) that was dissolved in blocking buffer. In addition, slides were also incubated with antibodies directed against the cortical layer markers, goat anti-Cux1 (sc-6327, 1:50; Santa Cruz Biotechnology, Inc. (Santa Cruz, CA)) and goat anti-FoxP2 (ab1307, 1:250; Abcam), which were used to localize cortical layers II/III and VI, respectively (30). The following day, the slides were washed and incubated with Cy3-conjugated donkey anti-rabbit (711-165-152, 1:1000; Jackson Immunoresearch) and Alexa 488-conjugated donkey anti-goat (A11055, 1:500; Invitrogen) for 1 h at room temperature. The slides were washed, and a coverslip was applied with Vectashield mounting medium (Vector Laboratories) that also contained 4′,6-diamidino-2-phenylindole (DAPI) to label cellular nuclei.

The slides were imaged on a Zeiss 510 confocal microscope using a ×63, 1.4 numerical aperture plan-apochromat lens by an investigator who was blinded to the genotypes of the sections. Scan settings were adjusted to utilize the full dynamic range of the photomultipliers and to provide a scan resolution of 97 nm/pixel and a slice thickness of 1 μm. The same scan settings were used for all of the images acquired within an experiment. We obtained images in the somatosensory cortex 1 μm below the surface of the tissue in cortical layers II/III and VI (as defined by Cux1 and FoxP2 staining) as well as in the subcortical white matter just below the edge of layer VI.

The images were reviewed by an investigator who was also blinded to the genotypes of the images. The background was defined as the average (among all of the slices imaged in a single experiment) of the mean pixel intensity of the white matter just below the somatosensory cortex. The same background value was used for all of the images in the experiment. We then calculated the mean background-subtracted intensity of α1 or α3 subunit staining and normalized those values to average wild type staining in layer II/III.

Immunoprecipitation—We incubated either 7.5 μg of anti-α1 subunit antibody, 2.5 μg of anti-α3 subunit antibody, or 7.5 or 2.5 μg of nonimmunized mouse or rabbit immunoglobulin (controls) with magnetic beads coupled to protein G (Invitrogen) in 500 μl of PBS for 1 h at 4 °C. The beads were washed and then incubated for 10 min with 500 μl of 0.2 M triethanolamine (pH 8.2) at room temperature. The antibodies were then covalently linked to the protein G by incubating with 20 mM dimethyl pimelimidate (Sigma-Aldrich) in 1 ml of 0.2 M triethanolamine (pH 8.2) at room temperature for 60 min. The coupling reaction was stopped with 50 mM Tris, pH 7.5.

The covalently coupled antibodies were incubated overnight at 4 °C with 350 μg of protein lysates that were prepared in a modified RIPA buffer (20 mM Tris, pH 7.4, 1% Triton X-100, 150 mM NaCl) that also contained protease inhibitor. After washing, the immunoprecipitated proteins were liberated from the antibodies by adding 50–100 μl of 1 M glycine in RIPA buffer (pH 3.0) and analyzed by Western blot.

Quantitative Real-time PCR—We measured relative abundances of α1 subunit and α3 subunit mRNA in wild type and Het$_{\alpha1}$KO mouse cortices essentially as described previously (31). Fresh cortices were dissected from wild type and Het$_{\alpha1}$KO mice, and total RNA was isolated using a commercial silica membrane column (Purelink). Using 200 ng of RNA, we generated corresponding cDNA with reverse transcriptase, using random hexamers as templates (Applied Biosystems). We performed quantitative real-time PCR using an Applied Biosystems 7900 with the TaqMan Universal Master Mix and with 6-carboxyfluorescein (FAM)-labeled probes (Applied Biosystems) for the α1 subunit (Mm00439046, spanning exon 9, which is deleted in Het$_{\alpha1}$KO) and the α3 subunit (Mm01294271) and a VIC-labeled probe (Applied Biosystems) for the endogenous control, β-actin (4352341E). We used the following real-time PCR conditions: We incubated at 95 °C for 10 min and then ran 40 cycles that consisted of denaturation at 95 °C for 15 s and annealing and extension at 60 °C for 60 s. We verified that Het$_{\alpha1}$KO did not change the expression of the endogenous control and then used the ΔΔ*Ct* cycle threshold method to calculate the effects of Het$_{\alpha1}$KO on the expression α1 and α3 subunit mRNA normalized to actin.

Endoglycosidase Digestion—Glycan analyses of proteins that traffic through the secretory pathway can determine the fraction of protein that is associated with the endoplasmic reticu-

lum (ER) as well as the fraction that has trafficked at least as far as the trans-Golgi (32, 33). Endoglycosidase H (endo-H) removes high mannose *N*-linked glycans attached to proteins in the endoplasmic reticulum but does not remove the complex glycans attached in the Golgi. Peptide:*N*-glycosidase F (PNGase F) removes all *N*-linked glycans. We obtained both endo-H and PNGase F from New England Biolabs. We made lysates of COS-7 cells transfected with $\alpha1\beta2\gamma2$ receptors (positive control) as well as wild type and Het$_{\alpha1}$KO cortices. We left the lysates undigested or treated them (20 μg of protein) with either endo-H or PNGase F for 2 h at 37 °C and then analyzed the digestion products on Western blot to determine the effects of Het$_{\alpha1}$KO on the fraction of total $\alpha1$ subunit associated with the ER.

Electrophysiology—Whole-cell patch clamp recordings were made at room temperature from layer VI pyramidal neurons in SI/II somatosensory cortex visualized with an upright Nikon eclipse FN-1 IR-DIC microscope. Neurons in the layer above the white matter showing a typical apical dendrite and large soma (smaller than the layer V neuronal somata) were chosen for recordings. The patch-pipette internal solution contained 135 mM CsCl, 10 mM EGTA, 10 mM HEPES, 5 mM ATP-Mg, and 5 mM QX-314 (pH 7.3, 290–295 mOsM) (24). The external solution was aCSF that also contained 6-nitro-sulfamoyl-benzo-quinoxaline-dione (NBQX) (20 μM) to block AMPA and kainate receptors. Filled electrodes had resistances of 2–4 megaohms. Serial resistance was continuously monitored during the experiments, and recordings with more than 25 megaohms or 20% change in serial resistance were discarded. Electrophysiological data were collected using a MultiClamp 700B amplifier (Molecular Devices Inc.) and Clampex version 10.2 software (Molecular Devices Inc.) with compensation for series resistance (70%) and cell capacitance, filtered at 2 kHz, and digitized at 20 kHz using a Digidata 1440A analog to digital converter (Molecular Devices Inc.).

Miniature inhibitory postsynaptic currents (mIPSCs) were recorded at −60 mV for at least 20 min in external solution that also contained tetrodotoxin (1 μM; Sigma-Aldrich) to block sodium channels. The mIPSCs were identified automatically offline using Clampfit version 10.2 and were confirmed visually, and the peak mIPSC amplitudes, interevent intervals, and 10–90% rise times were identified. The current decay of each mIPSC was fit to a single exponential, and the decay constant (τ) was calculated. We excluded mIPSCs with a peak amplitude less than 1 pA, a decay constant less than 1 ms or greater than 1000 ms, or a rise time greater than 10 ms. We created cumulative histograms for the peak amplitudes, rise times, and decay constants for all of the mIPSCs obtained from all the neurons of the same genotype. We also calculated the mean peak amplitude, event interval, rise time, and decay constant for all of the mIPSCs recorded from each neuron, averaged these mean values among all of the recorded cells, and then compared the wild type and Het$_{\alpha1}$KO averaged values using a two-tailed *t* test. In addition, we created averaged mIPSC tracings for each neuron, fit the current decay of the average traces with one or two time constants (τ_1 and τ_2), and calculated the weighted decay constant (τ_w) as $(\tau_1 \times A_1 + \tau_2 \times A_2)/(A_1 + A_2)$, where A_1 and A_2 represent the amplitudes of the corresponding decay constants.

Evoked inhibitory postsynaptic currents (eIPSCs) were performed in external solution that did not contain tetrodotoxin. To record eIPSCs, we placed a concentric stimulation electrode close to the recorded neuron. We started stimulating at 0.1 V every 20 s and increased the voltage until maximal monosynaptic responses were achieved; the voltage was then reduced to produce half-maximal monosynaptic responses. We recorded 10 eIPSC traces from each neuron (base line) before adding either of the benzodiazepine agonists diazepam (1 μM) or zolpidem (100 nM; Sigma-Aldrich). Five minutes after adding benzodiazepine agonist, we recorded an additional 10 eIPSC traces. The traces recorded before or after benzodiazepine agonist were averaged. We identified the peak current amplitude before and after the addition of drug and also fit the decay phase of the averaged eIPSCs with 1–2 time constants and calculated the weighted decay constant (τ_w) as described above.

Analysis of GABA$_A$R Endocytosis/Recycling—We determined the effects of Het$_{\alpha1}$KO on GABA$_A$R endocytosis/recycling from the plasma membrane in layer VI pyramidal neurons by adapting two previously published methods that measured neurotransmitter receptor endocytosis in brain slices (29, 34–38). We first tested the effects of the membrane-permeable reagent, 3-hydroxy-naphthalene-2-carboxylic acid (dynasore; Sigma-Aldrich), a compound that inhibits dynamin's GTPase activity and thus inhibits dynamin-mediated endocytosis. We measured mIPSCs in layer VI pyramidal neurons for a 5-min base-line period as described above. We then added dynasore to the bath (final concentration 80 μM, 0.2% DMSO) and measured mIPSCs for an additional 20 min. We averaged the mIPSC peak amplitudes in 1-min blocks before and after the dynasore addition and determined the time-dependent change in mIPSC amplitudes in wild type and Het$_{\alpha1}$KO neurons.

Next, we tested the effects of intracellular administration of dynamin inhibitory peptide (P4 peptide, Tocris Bioscience), a membrane-impermeable inhibitor of dynamin-mediated endocytosis that acts by blocking the binding of dynamin to amphiphysin. We added P4 peptide (50 μM) to the patch pipette internal solution and measured mIPSCs in layer VI pyramidal neurons for 25 min. As above, we determined the effect of Het$_{\alpha1}$KO on the time-dependent changes in mIPSC peak amplitudes.

Data Analysis and Statistics—Statistical analyses were performed using the R 2.12.2 Statistical Package for Windows (R Foundation for Statistical Computing). All results are presented as the means ± S.E. When making two comparisons, the statistical significance of averaged values was assessed using the single-sample or independent samples *t* test, as appropriate. We used two-way analysis of variance to test the significance of differences in α subunit staining between wild type and Het$_{\alpha1}$KO cortices in cortical layers II/III and VI. In addition, we used the two-sample Kolmogorov-Smirnov (K-S) test to compare the distributions of wild type and Het$_{\alpha1}$KO mIPSC peak amplitudes, interevent intervals, 10–90% rise times, and decay constants. *p* values less than 0.05 were considered statistically significant, and the Bonferroni-corrected *p* value was used if appropriate.

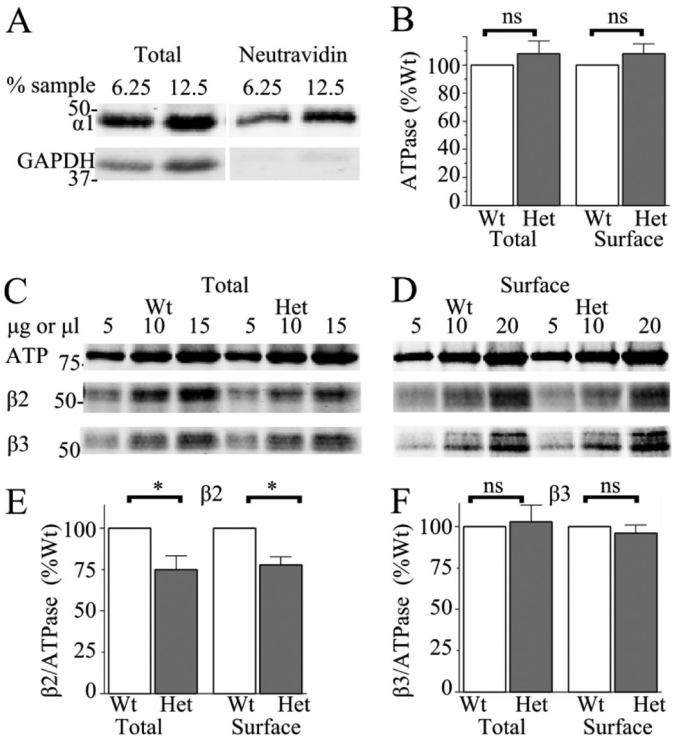

FIGURE 1. **Het$_{\alpha 1}$KO reduced β2 but not β3 subunit expression.** *A*, we treated wild type brain slices with a membrane-impermeable biotinylation reagent and purified the biotinylated proteins with immobilized neutravidin. Equivalent fractions (6.25 and 12.5%) of the total cortical lysates and neutravidin-purified material were analyzed on Western blots and stained for the integral membrane protein, α1 subunit, and the cytosolic protein, GAPDH (*A*). Biotinylation and neutravidin purification was selective for the α1 subunit, relative to GAPDH, with 45 $\pm$ 6% (n = 4) of the total α1 subunit and only 8 $\pm$ 2% (n = 5) of total GAPDH in the neutravidin-purified fraction. *B*, brain slices from wild type and Het$_{\alpha 1}$KO mice were biotinylated, and the cortical lysates were purified with immobilized neutravidin. Equal masses of total lysate and neutravidin-purified material were analyzed by Western blot. Het$_{\alpha 1}$KO did not significantly alter the total (108 $\pm$ 9%, n = 6) or surface (108 $\pm$ 7%, n = 4) expression of the loading control protein, the Na^+/K^+ ATPase α subunit. *C–F*, we analyzed 5, 10, and 15 μg of total (*C*) and 5, 10, and 20 μl of surface (*D*) cortical protein on Western blot and stained for the Na^+/K^+ ATPase α subunit (*ATP*) and the β2 and β3 subunits. Graphs (*E* and *F*) depict the relative amounts of ATPase-normalized β2 and β3 subunits from Het$_{\alpha 1}$KO mice compared with those of wild type. Het$_{\alpha 1}$KO reduced total and surface β2 subunit expression to 75 $\pm$ 8% (n = 8, p = 0.019) and 78 $\pm$ 5% (n = 8, p = 0.003) compared with wild type. Het$_{\alpha 1}$KO did not significantly change total (102 $\pm$ 8%, n = 6, p = 0.796) or surface (96 $\pm$ 5%, n = 8, p = 0.458) β3 subunit expression. *Error bars*, S.E.

RESULTS

Het$_{\alpha 1}$KO Reduces β2 but Not β3 Subunit Expression—All known functional GABA$_A$Rs contain two β subunits, which exist as β1, β2, and β3 subunit isoforms (6). Therefore, we determined the effects of Het$_{\alpha 1}$KO on total and surface β1–3 subunit expression as a measure of the effects of Het$_{\alpha 1}$KO mutation on the expression of functional GABA$_A$Rs. We measured cortical β subunit expression using brain slice biotinylation assays and Western blots, a semiquantitative technique that can reliably separate surface and total protein and allows for direct evaluation of the linearity of protein detection (27–29, 33). We first verified that the biotinylation reagent was selective for membrane proteins by measuring the amount of the cytoplasmic protein, GAPDH, in the neutravidin-purified and unpurified samples (Fig. 1*A*). We next confirmed that Het$_{\alpha 1}$KO did not alter the total or surface expression of the loading control protein, the Na^+/K^+ ATPase α subunit (Fig. 1*B*). We verified that the neutravidin beads were not saturated with biotinylated protein by incubating increasing masses of biotinylated lysate with neutravidin beads and detecting proportional increases in detected protein on Western blot (not shown).

Although our immunoblots reliably detected mouse β1 subunit recombinantly expressed in COS-7 cells, we did not detect total or surface β1 subunit in wild type or Het$_{\alpha 1}$KO cortices (not shown), a result that suggests that the β1 subunit is not highly expressed in cortices of mice of this age. We found that Het$_{\alpha 1}$KO reduced total β2 subunit expression to 75 $\pm$ 8% that of wild type (Fig. 1, *C* and *E*; n = 8; p = 0.019 *versus* 100%) and reduced surface β2 subunit expression to 78 $\pm$ 5% that of wild type (Fig. 1, *D* and *E*; n = 8; p = 0.003 *versus* 100%). However, Het$_{\alpha 1}$KO did not change the total (Fig. 1, *C* and *F*; 102 $\pm$ 8%; n = 6; p = 0.796 *versus* 100%) or surface (Fig. 1, *D* and *F*; 96 $\pm$ 5%; n = 8; p = 0.458 *versus* 100%) expression of the β3 subunit. The absence of an effect on β3 subunit expression and the modest reduction of β2 subunit expression suggest that Het$_{\alpha 1}$KO causes only a small reduction in the expression of functional GABA$_A$Rs of all isoforms. This result suggests that neurons partially compensate for the heterozygous loss of the α1 subunit by increasing expression from the wild type α1 subunit allele or increasing expression of other α subunit isoforms. In addition, the selective reduction of β2 but not β3 subunit could suggest preferential assembly of GABA$_A$Rs with the β3 subunit in Het$_{\alpha 1}$KO cortices.

Het$_{\alpha 1}$KO Reduced Total α1 Subunit Expression but Increased Its Relative Surface Expression—Using Western blots, previous investigators found that Het$_{\alpha 1}$KO reduced total cortical α1 subunit protein expression (14). Here, we conducted immunofluorescence studies to determine if the reduction in α1 subunit expression was homogenous without substantial cell-to-cell variability and if it occurred to a similar extent in the upper (II/III) and lower (VI) layers of the cortex. We conducted these immunofluorescence experiments in the somatosensory cortex because this is the area thought to initiate absence seizures in rodents (39, 40).

Control experiments using cortices from homozygous α1 subunit deletion mice demonstrated the specificity of the anti-α1 subunit antibody and that the images had similar background levels of staining as the white matter of wild type cortex (not shown). Immunofluorescence studies of wild type and Het$_{\alpha 1}$KO cortices revealed that Het$_{\alpha 1}$KO reduced total α1 subunit expression homogeneously with no visible cell-to-cell variability (Fig. 2, *A–D*, $n \geq 8$). Moreover, Het$_{\alpha 1}$KO reduced total α1 subunit expression in both layer II/III and layer VI (Fig. 2*G*, p = 0.001). For both genotypes, there was less α1 subunit expressed in layer VI than layer II/III. However, there was no significant interaction between the effects of genotype and cortical layer in influencing α1 subunit expression (Fig. 2*G*, p = 0.113, two-way analysis of variance).

It should be emphasized that although Het$_{\alpha 1}$KO caused an apparent homogenous reduction of α1 subunit expression, we cannot exclude the possibility that Het$_{\alpha 1}$KO causes differential effects among/between populations of cortical neurons that are relatively small in number. For example, although pyramidal

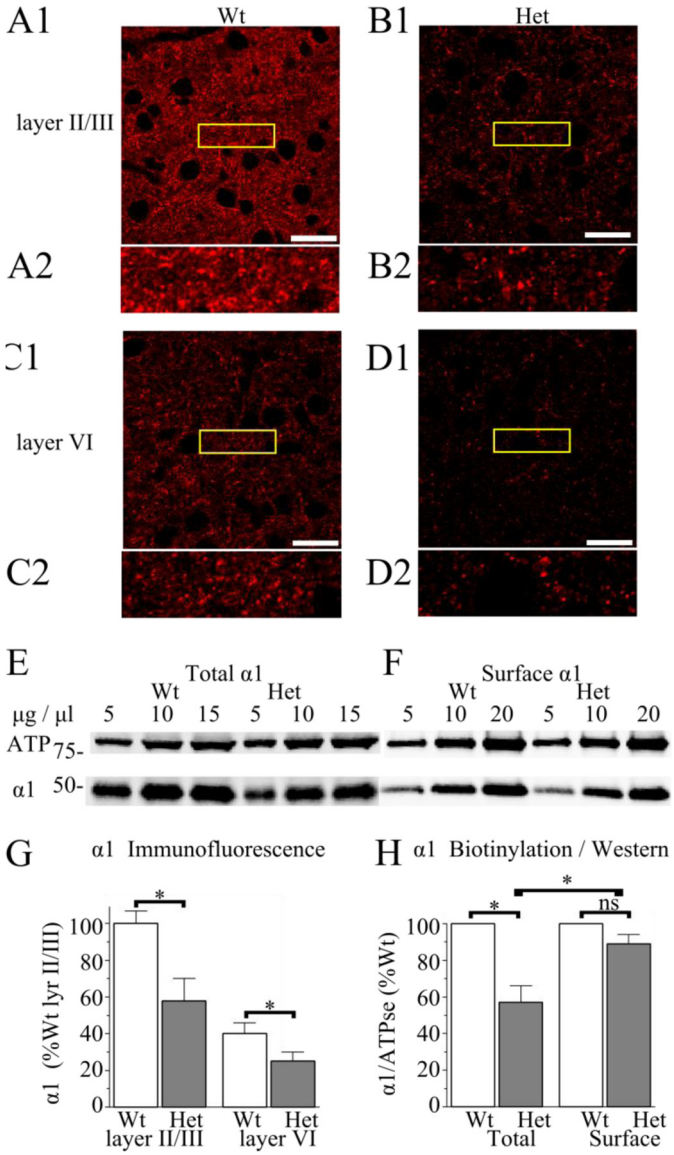

FIGURE 2. **Het$_{\alpha1}$KO reduced total α1 subunit expression and increased the relative surface α1 subunit expression.** *A–D,* immunofluorescence images of α1 subunit staining in wild type (*A* and *C*) and Het$_{\alpha1}$KO mice (*B* and *D*) in layers II/III (*A* and *B*) and VI (*C* and *D*) of the somatosensory cortex (*white scale bar*, 20 μm; $n \geq 8$). The *yellow boxed areas* are displayed on a *magnified scale below* each image (*A2–D2*). Het$_{\alpha1}$KO reduced α1 subunit expression in both layer II/III and layer VI with no apparent cell-to-cell variability in each microscopic image. Quantification of total α1 subunit expression is presented in the graph in *G*. In both genotypes of mice, there was greater α1 subunit expression in layer II/III than in layer VI ($p < 0.001$). Het$_{\alpha1}$KO significantly reduced total α1 subunit expression in both cortical layers ($p = 0.001$), and there was no significant interaction between the effects of the genotype and the cortical layer on α1 subunit expression ($p = 0.113$, two-factor analysis of variance). *E* and *F*, biotinylation and Western blot experiments used to quantify the effects of Het$_{\alpha1}$KO on surface and total α1 subunit expression. We analyzed 5, 10, and 15 μg of total (*E*) and 5, 10, and 20 μl of surface (*F*) protein on Western blot and stained for the GABA$_A$R α1 subunit and Na^+/K^+ ATPase α subunit. Graphs (*H*) depict the relative amounts of ATPase-normalized α1 subunits from Het$_{\alpha1}$KO mice compared with those of wild type. Het$_{\alpha1}$KO caused a greater reduction in total (62 ± 8% wild type, $n = 8$) than in surface (89 ± 5% wild type, $n = 5$, $p = 0.015$) α1 subunit expression and thus increased the relative surface expression of the α1 subunit. *Error bars*, S.E.

neurons comprise 80% of cortical neurons, the remaining 20% are composed of several different types of interneurons (41). It is possible that Het$_{\alpha1}$KO causes different effects on α1 subunit expression in one or more of these different types of interneurons than it does in the pyramidal neurons.

We performed cell surface biotinylation studies to quantify the effect of Het$_{\alpha1}$KO on surface α1 subunit expression and to determine if Het$_{\alpha1}$KO cortices compensated for the reduction of total α1 subunit protein by increasing the fraction of residual total α1 subunit expressed on the cell surface (*i.e.* increasing the relative surface expression). We found that total α1 subunit protein expression in Het$_{\alpha1}$KO cortices was 62 ± 8% that of wild type (Fig. 2, *E* and *H*; $n = 8$; $p = 0.002$ *versus* 100%), a value consistent with previous Western blots (14) as well as our immunofluorescence studies. However, Het$_{\alpha1}$KO caused a significantly smaller effect on cell surface α1 subunit protein expression (Fig. 2, *F* and *H*; 89 ± 5%; $n = 5$; $p = 0.015$ *versus* total expression). This result suggests that Het$_{\alpha1}$KO partially compensates for the reduction of total α1 subunit protein expression by increasing its relative surface expression.

Het$_{\alpha1}$KO Increased the Total and Surface Expression of the α3 Subunit—In addition to α1 subunit-containing GABA$_A$Rs, adult wild type cortices also express α3 and α2 subunit-containing receptors at GABAergic synapses, albeit at lower abundances (42–44). Therefore, we determined the effects of Het$_{\alpha1}$KO on total and surface expression of the α3 and α2 subunits to determine if either of these other synaptic-type α subunits could substitute for α1 on the cell surface.

We determined the effects of Het$_{\alpha1}$KO on the distribution of α3 subunit in layers II/III and VI in the somatosensory cortex using immunofluorescence. Control experiments on cortices from the α3 subunit deletion mouse demonstrated that the anti-α3 subunit antibody was specific for the α3 subunit (not shown). We found that Het$_{\alpha1}$KO increased total α3 subunit staining in both layers II/III and VI with no visible cell-to-cell variability (Fig. 3, *A–D* and *G*; $n \geq 6$; $p < 0.001$). Brain slice biotinylation and Western blot assays demonstrated that Het$_{\alpha1}$KO increased total and surface α3 subunit expression to 138 ± 18% (Fig. 3, *E* and *H*, $n = 10$, $p = 0.016$ *versus* 100%) and 174 ± 24% (Fig. 3, *F* and *H*, $n = 7$; $p = 0.020$ *versus* 100%) the levels of wild type expression, respectively. These results demonstrated that Het$_{\alpha1}$KO also partially compensates for the loss of α1 subunit by increasing the total and surface protein expression of the α3 subunit. There was no significant change in the α2 subunit expression (Fig. 3, *I* and *J*).

Het$_{\alpha1}$KO Altered the Association of α1 and α3 Subunits—GABA$_A$R pentamers contain two α subunits, which can be of the same or different isoforms (45, 46). Because Het$_{\alpha1}$KO altered the expression of the α1 and α3 subunits, we next determined whether it also altered the association of these two subunits.

We demonstrated that anti-α1 and anti-α3 subunit antibodies were specific for their respective subunits and that control immunoglobulin from nonimmunized mice and rabbits did not immunoprecipitate either subunit from homogenized mouse cortex (Fig. 4, *A* and *B*). Wild type and Het$_{\alpha1}$KO cortical lysates were then immunoprecipitated using the anti-α1 or -α3 subunit antibodies, and the immunoprecipitated material was analyzed on Western blot with staining for both the α1 and α3 subunits (Fig. 4, *C–F*). Immunoprecipitation using the α1 subunit antibody produced 68 ± 11% α1 subunit from the

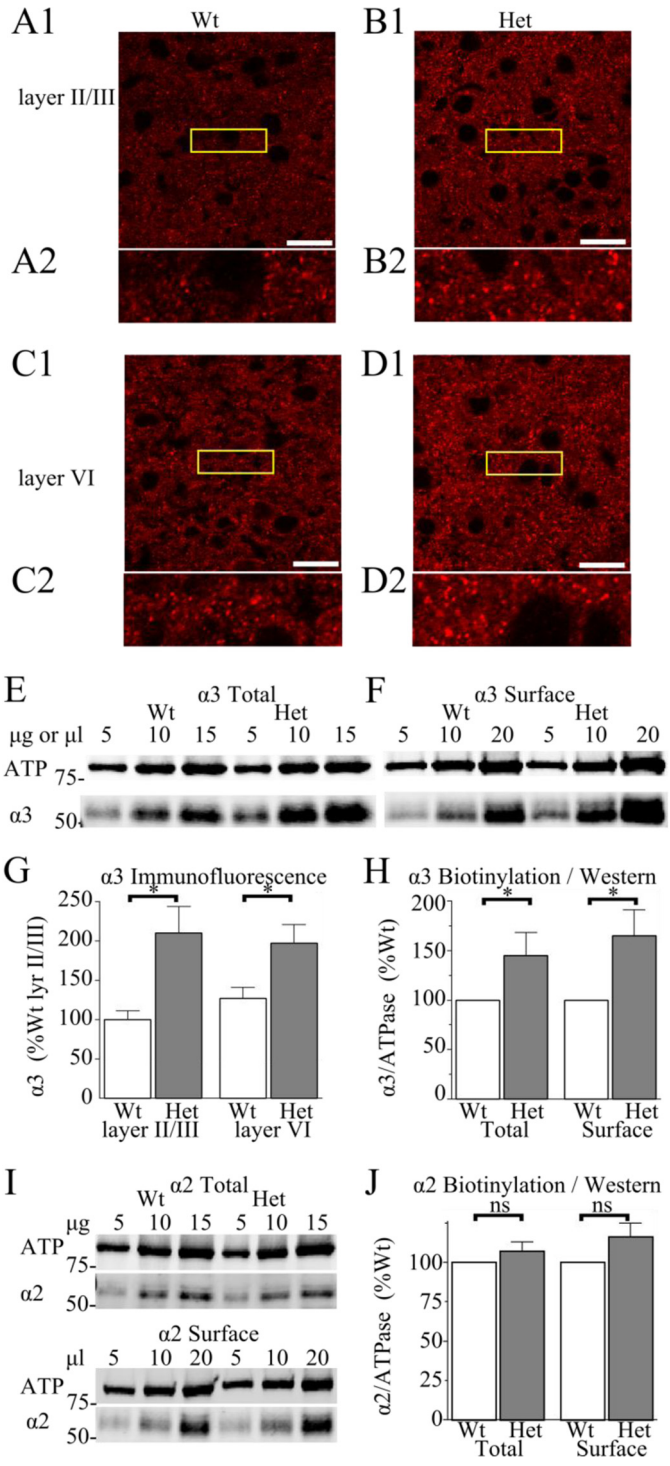

FIGURE 3. **Het$_{\alpha1}$KO increased the total and surface expression of the α3 subunit but not the α2 subunit.** *A–D*, immunofluorescence images of α3 subunit staining in wild type (*A* and *C*) and Het$_{\alpha1}$KO (*B* and *D*) mice in layers II/III (*A* and *B*) and VI (*C* and *D*) of the somatosensory cortex (*white scale bar*, 20 μm, $n \geq 6$). The *yellow boxed areas* are displayed on a *magnified scale below* each image (*A2–D2*). Quantification of the total α3 subunit staining (*G*) showed that Het$_{\alpha1}$KO increased α3 subunit expression ($p < 0.001$) in both layer II/III and layer VI and that there was no effect of the cortical layer on α3 subunit expression ($p = 0.720$, two-factor analysis of variance). We performed biotinylation assays and Western blots to quantify the amount of total and surface α3 subunit. We analyzed 5, 10, and 15 μg of total (*E*) and 5, 10, and 20 μl of surface (*F*) cortical protein on Western blot and stained for the α3 subunit as well as the ATPase α subunit. The graph (*H*) depicts the relative amount of ATPase-normalized α3 subunit from Het$_{\alpha1}$KO mice compared with those of wild type. Het$_{\alpha1}$KO increased total α3 subunit expression to 138 ± 18% ($n = 10$, $p = 0.016$) and surface α3 subunit expression to 174 ± 24% ($n = 7$, $p = 0.020$). Biotinylation assays and Western blots (*I–J*) demonstrated that Het$_{\alpha1}$KO did not significantly change total (105 ± 4%, $n = 4$, $p = 0.389$) or surface (117 ± 7%, $n = 5$, $p = 0.081$) α2 subunit expression. *Error bars*, S.E.

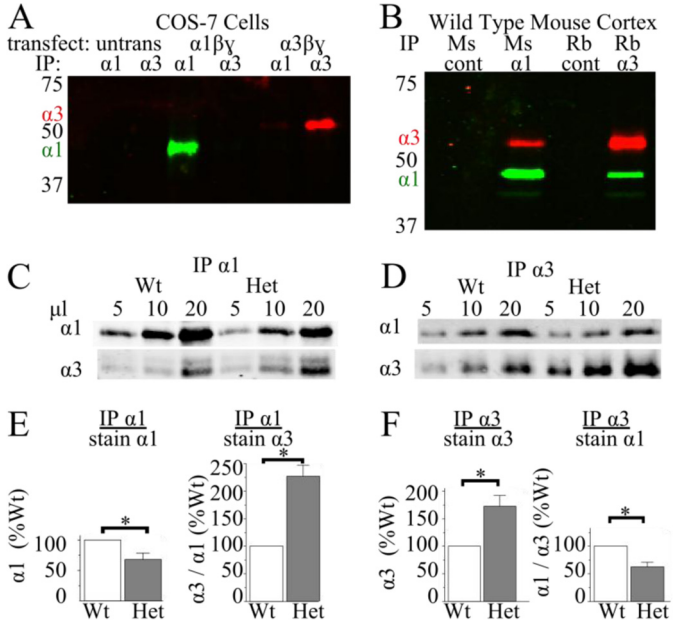

FIGURE 4. **Het$_{\alpha1}$KO altered the association of α1 and α3 subunits.** *A*, COS-7 cells were left untransfected or were transfected with α1β2γ2 or α3β2γ2 GABA$_A$R ($n = 3$). Cellular lysates were immunoprecipitated (*IP*) with either the α1 or α3 subunit, and the products were analyzed by Western blot. The blots were probed with the anti-α1 subunit antibody (*green*) and the anti-α3 subunit antibody (*red*). Neither the α1 nor α3 antibody immunoprecipitated proteins from untransfected cells. The α1 subunit antibody but not the anti-α3 subunit antibody immunoprecipitated the α1 subunit protein from the cells expressing α1β2γ2 receptors, and the α3 subunit antibody but not the α1 subunit antibody immunoprecipitated α3 subunit protein from the cells expressing α3β2γ2 receptors. *B*, cortical lysates from wild type mice were immunoprecipitated with the mouse α1 subunit antibody (*Ms* α1), the rabbit α3 subunit antibody (*Rb* α3), or control immunoglobulin from nonimmunized mice (*Ms cont*) or rabbits (*Rb cont*). Immunoprecipitated material was analyzed by Western blot and stained for the α1 (*green*) or α3 (*red*) subunit. The anti-α1 and anti-α3 subunit antibodies coimmunoprecipitated α1 and α3 subunits, but neither the mouse nor rabbit control immunoglobulin immunoprecipitated either subunit. *C–F*, total protein from wild type and Het$_{\alpha1}$KO cortices was immunoprecipitated with antibodies directed against the α1 or α3 subunits. Immunoprecipitated material (5, 10, and 20 μl) was analyzed on Western blot, which was stained with both the α1 and α3 subunit antibodies (*C* and *D*). Immunoprecipitation using the anti-α1 subunit antibody (*C* and *E*) recovered 68 ± 11% as much α1 subunit from Het$_{\alpha1}$KO cortex as compared with wild type cortex ($n = 5$, $p = 0.039$), and, when normalized to recovered α1 subunit, co-immunoprecipitated 227 ± 20% as much α3 subunit from Het$_{\alpha1}$KO cortex as from wild type cortex ($n = 4$, $p = 0.008$). Immunoprecipitation using the anti-α3 subunit antibody (*D* and *F*) recovered 173 ± 19% as much α3 subunit from Het$_{\alpha1}$KO as from wild type cortex ($n = 5$, $p = 0.020$) and co-immunoprecipitated 63 ± 8% as much normalized α1 subunit from Het$_{\alpha1}$KO as from wild type cortex ($n = 4$, $p = 0.008$). *Error bars*, S.E.

Het$_{\alpha1}$KO lysate compared with the wild type lysate ($n = 5$; $p = 0.039$ *versus* 100%), an amount consistent with the effect of Het$_{\alpha1}$KO on total α1 subunit expression demonstrated in Fig. 2. When normalized to the amount of recovered α1 subunit, immunoprecipitation with the α1 subunit antibody co-immunoprecipitated 227 ± 20% α3 subunit protein from the Het$_{\alpha1}$KO lysate compared with the wild type lysate ($n = 4$; $p = 0.008$ *versus* 100%). This result suggests that, in addition to Het$_{\alpha1}$KO decreasing the total expression of α1 subunit protein, it also decreased the fraction of α1 subunit incorporated in

$\alpha1\beta\gamma$ receptors and increased the fraction in $\alpha1\alpha3\beta\gamma$ receptors.

Immunoprecipitation using the $\alpha3$ subunit antibody produced 173 ± 19% $\alpha3$ subunit from Het$_{\alpha1}$KO wild type expression ($n = 5$; $p = 0.020$ *versus* 100%), a result consistent with the increase in $\alpha3$ subunit expression in Het$_{\alpha1}$KO mice demonstrated in Fig. 3. Immunoprecipitation of the $\alpha3$ subunit coimmunoprecipitated 63 ± 8% normalized $\alpha1$ subunit ($n = 4$; $p = 0.022$ *versus* 100%). These data suggest that in addition to Het$_{\alpha1}$KO increasing the expression of the $\alpha3$ subunit, it also decreased the fraction of $\alpha3$ subunits incorporated into $\alpha1\alpha3\beta\gamma$ receptors and increased the fraction of $\alpha3$ subunits that are incorporated into $\alpha3\beta\gamma$ receptors.

Het$_{\alpha1}$KO Altered GABAergic Synaptic Currents and Their Response to Benzodiazepine Agonists—GABA$_A$Rs that contain different α subunit isoforms possess distinct physiological and pharmacological properties. In particular, GABA$_A$Rs that contain $\alpha3$ subunits exhibit slower current decay times, increased current rise times, and a reduced sensitivity for GABA (larger EC$_{50}$) as compared with $\alpha1$-containing GABA$_A$R (7, 47, 48). In addition, diazepam enhances currents in GABA$_A$Rs with the stoichiometry of $\alpha_x\beta\gamma2$ (where x is 1, 2, 3, or 5), whereas zolpidem selectively enhances currents in $\alpha1\beta\gamma2$ GABA$_A$Rs with a greater potency than $\alpha2\beta\gamma2$ or $\alpha3\beta\gamma2$ GABA$_A$R (49–52). Therefore, because our biochemical studies demonstrated that Het$_{\alpha1}$KO altered the surface expression and composition of GABA$_A$Rs, we next examined the effects of Het$_{\alpha1}$KO on synaptic GABA$_A$R physiology and pharmacology.

We examined the effects of Het$_{\alpha1}$KO on the mIPSCs recorded from somatosensory cortex layer VI pyramidal neurons, the brain region and cortical layer thought to initiate absence seizures (40) and that projects to the thalamus, the brain region thought to sustain the oscillations (53). Representative traces are presented in Fig. 5, *A* and *B* (wild type, $n = 11$; Het$_{\alpha1}$KO, $n = 10$). Het$_{\alpha1}$KO significantly reduced the magnitude of the average peak mIPSC amplitude (Fig. 5, *C* and *D*) both when all mIPSCs were analyzed together in a cumulative histogram (K-S test $p < 0.001$) and when averaged among individual neurons (wild type, −43 ± 4.1 pA; Het$_{\alpha1}$KO, −32 ± 2.5 pA; $p = 0.032$).

In addition to reducing the peak current amplitudes, Het$_{\alpha1}$KO also altered the time course of mIPSC kinetics. First, Het$_{\alpha1}$KO increased the 10–90% rise time from 1.8 ± 0.15 to 2.4 ± 0.20 ms (not shown; K-S test, $p < 0.001$; *t* test, $p = 0.024$). Second, Het$_{\alpha1}$KO increased the time course of mIPSC decay (Fig. 5, *E* and *F*). We fit the time course of current decay of each mIPSC to a single exponential and calculated the decay time constant, τ, for each mIPSC. When analyzed in cumulative histograms (K-S test, $p < 0.001$) and when averaged among neurons ($p = 0.034$), Het$_{\alpha1}$KO significantly prolonged the decay time constant (wild type, 24 ± 0.9 ms; Het, 27 ± 1.3 ms). Importantly, there were no correlations among the peak current amplitudes, the rise times, and the decay constants, a finding that suggests that the effect of Het$_{\alpha1}$KO on these values results from alterations in GABA$_A$R physiology rather than a redistribution of GABA$_A$R synapses to other neuronal locations (*e.g.* to locations more distal from the soma that could also produce apparent changes in current kinetic parameters by introducing space clamp error).

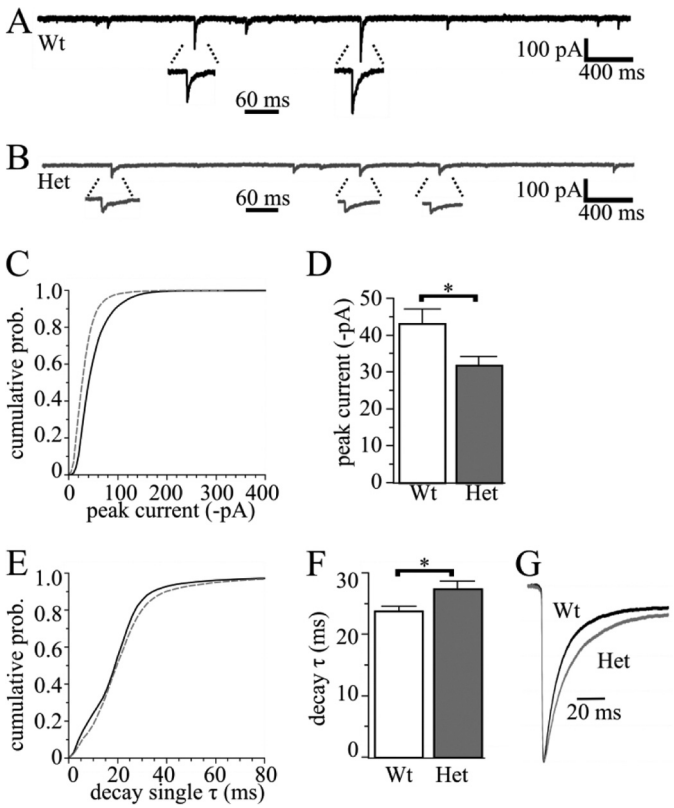

FIGURE 5. **Het$_{\alpha1}$KO decreased the mIPSC peak amplitudes and altered the time course of current kinetics in layer VI pyramidal neurons.** *A* and *B* depict, respectively, representative mIPSC tracings from cortical layer VI pyramidal wild type ($n = 11$, *black*) and Het$_{\alpha1}$KO ($n = 10$, *gray*) neurons. The *insets* on the *traces* depict mIPSCs on an expanded time scale to demonstrate the time course of current decay. *C* and *E*, cumulative histograms summarizing the individual mIPSC absolute peak current amplitudes and decay time constants (single τ). Compared with wild type (*black solid line*), Het$_{\alpha1}$KO (*gray dashed line*) reduced the peak current amplitudes and increased the time course of current decay (K-S test, $p < 0.001$). We calculated the average amplitude and decay constant for each neuron individually. The bar graphs (*D* and *F*) depict the mean of the averaged amplitude and τ values and demonstrate that Het$_{\alpha1}$KO reduced the absolute mean peak amplitude (wild type, −43 ± 4.1 pA; Het$_{\alpha1}$KO, −32 ± 2.5 pA; $p = 0.032$) and prolonged the mean decay time constant (wild type, 24 ± 0.9 ms; Het, 27 ± 1.3 ms; $p = 0.034$). We averaged the mIPSC traces separately for each neuron with normalized amplitudes, calculated the weighted time constants of current decay (τ_w), and depicted specimen traces in *G*. Het$_{\alpha1}$KO increased the weighted time constant (τ_w) from 12.7 ± 1.0 to 17.4 ± 1.6 ms ($p = 0.024$). *Error bars*, S.E.

GABA$_A$R current decay is often fit to the sum of two exponentials, a process that difficult to perform accurately if applied to each mIPSC individually. Therefore, we constructed averaged mISPC traces from each neuron and fit the current decay to one or two exponentials and calculated the weighted time constant, τ_w. We found that Het$_{\alpha1}$KO increased τ_w from 12.7 ± 1.0 ms to 17.4 ± 1.6 ms (Fig. 5*G*, $p = 0.024$). These effects of Het$_{\alpha1}$KO on mIPSC amplitude, rise time, and decay are consistent with the changes in GABA$_A$R expression and composition revealed in our biochemistry experiments.

We also determined the effects of Het$_{\alpha1}$KO on mIPSC frequency. Interestingly, although Het$_{\alpha1}$KO reduced the mIPSC frequency when all mIPSCs were analyzed in a cumulative histogram (not shown; K-S test, $p < 0.001$), there was sufficient variation in the average mIPSC frequencies that this difference

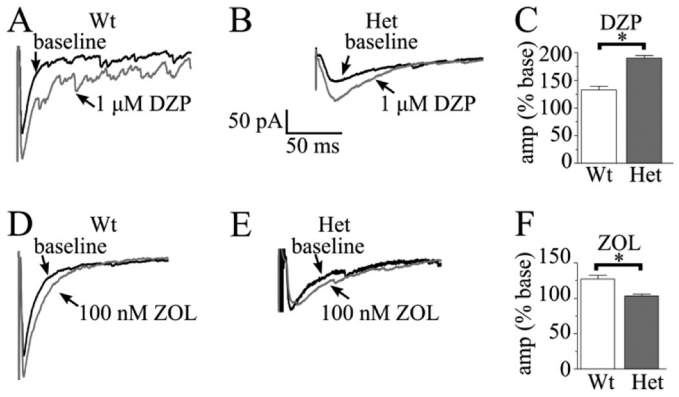

FIGURE 6. **Het$_{\alpha1}$KO altered the responses of cortical pyramidal neurons to benzodiazepine agonists.** We recorded eIPSCs in the absence (*black*) and presence (*gray*) of the benzodiazepine agonists, diazepam (1 μM; *A–C*) and zolpidem (100 nM; *D–F*) in wild type (*A* and *D*) and Het$_{\alpha1}$KO (*B* and *E*) layer VI pyramidal neurons. Diazepam increased the eIPSC amplitude in both wild type (133 ± 6.8%, $n = 6$, $p = 0.005$ *versus* 100%) and Het$_{\alpha1}$KO neurons (190 ± 5.1%, $n = 5$, $p = 0.006$ *versus* 100%) but had a greater effect on Het$_{\alpha1}$KO than wild type neurons (*C*, $p = 0.007$ wild type *versus* Het$_{\alpha1}$KO). Zolpidem increased eIPSC amplitudes in wild type (127 ± 4.1%, $n = 8$, $p < 0.001$ *versus* 100%) but not Het$_{\alpha1}$KO neurons (105 ± 3.1%; $n = 7$; $p = 0.130$ *versus* 100%, $p = 0.001$ *versus* wild type). *Error bars*, S.E.

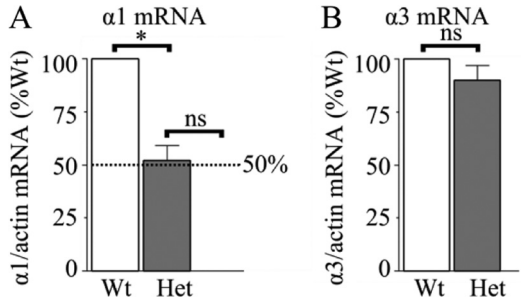

FIGURE 7. **Het$_{\alpha1}$KO did not increase α3 subunit mRNA expression or α1 subunit mRNA driven from the wild type allele.** We extracted total mRNA from wild type and Het$_{\alpha1}$KO cortices and performed quantitative real-time PCR with probes that amplified the α1 (*A*) and α3 (*B*) subunits as well as actin, the endogenous control. Het$_{\alpha1}$KO reduced α1 subunit mRNA expression to 52 ± 7% that of wild type ($n = 6$; $p = 0.001$ *versus* 100%, $p = 0.750$ *versus* 50%) and did not significantly change α3 subunit mRNA expression (90 ± 7%, $n = 6$, $p = 0.230$ *versus* 100%). *Error bars*, S.E.

was not statistically significant when averaged among individual neurons (not shown; wild type, 3.0 ± 0.59 Hz; Het$_{\alpha1}$KO, 2.3 ± 0.39 Hz; $p = 0.381$). Further studies will be necessary to determine if, in addition to altering GABA$_A$R expression and composition, Het$_{\alpha1}$KO also affects synaptogenesis or GABA release from presynaptic interneurons, processes that can alter mIPSC frequency.

Next, we studied the effects of the benzodiazepine site agonists, diazepam and zolpidem, on eIPSCs from layer VI pyramidal neurons in wild type and Het$_{\alpha1}$KO cortices. In pharmacological experiments, the study of eIPSCs allows one to more rapidly characterize pre- and postdrug GABAergic physiology than could be achieved with the study of mIPSCs. We found that 1 μM diazepam increased the peak eIPSC amplitudes in both wild type (133 ± 6.8%; $n = 6$; $p = 0.005$ *versus* 100%) and Het$_{\alpha1}$KO neurons (190 ± 5.1%; $n = 5$; $p = 0.006$ *versus* 100%) but had a significantly greater effect on Het$_{\alpha1}$KO than wild type neurons (Fig. 6, *A–C*, $p = 0.021$ wild type *versus* Het$_{\alpha1}$KO). Because diazepam works, in part, by reducing the EC$_{50}$ of GABA$_A$Rs for GABA, the greater response of Het$_{\alpha1}$KO than wild type neurons for diazepam suggests that Het$_{\alpha1}$KO neurons express receptors with a lower GABA sensitivity, such as α3 subunit-containing receptors.

In seven of the eight wild type neurons recorded, 100 nM zolpidem had a similar effect as diazepam on peak eIPSC amplitudes (Fig. 6, *D* and *F*, 126 ± 4.3%; $n = 7$; $p < 0.001$ *versus* 100%). However, in one wild type neuron, zolpidem caused an atypically large increase in eIPSC amplitude (574%), and thus, although the direction of the effect was expected for a wild type neuron, its abnormally large magnitude required that it be excluded from analysis. In contrast to wild type neurons, zolpidem did not significantly change eIPSC amplitudes in Het$_{\alpha1}$KO neurons (Fig. 6, *E* and *F*, 105 ± 3.1%; $n = 7$; $p = 0.130$ *versus* 100%, $p = 0.001$ *versus* wild type). Because zolpidem selectively enhances the current of α1 subunit-containing GABA$_A$R, these results suggest that Het$_{\alpha1}$KO substitutes non-α1 subunit-containing GABA$_A$R for α1βγ receptors.

These studies of the consequences of Het$_{\alpha1}$KO on cortical neuron synaptic physiology and pharmacology are consistent with our biochemical experiments showing that Het$_{\alpha1}$KO altered GABA$_A$R expression and composition. Moreover, they also suggest a mechanism by which Het$_{\alpha1}$KO causes cortical hyperexcitability and seizures.

Het$_{\alpha1}$KO Did Not Increase α3 Subunit mRNA Expression or α1 Subunit mRNA Driven from the Wild Type Allele—We next used quantitative real-time PCR to determine if Het$_{\alpha1}$KO caused compensatory changes in α1 or α3 mRNA expression. Het$_{\alpha1}$KO did not alter the expression of actin mRNA (endogenous control) but reduced actin-normalized α1 subunit mRNA expression to 52 ± 7% ($n = 6$; $p = 0.001$ *versus* 100%; $p = 0.750$ *versus* 50%) that of wild type, an amount consistent with the functional heterozygous deletion of the α1 subunit gene without mRNA compensation from the wild type α1 subunit (Fig. 7*A*). Het$_{\alpha1}$KO also did not elicit compensation in the expression of α3 subunit mRNA (90 ± 7%, $n = 6$; $p = 0.230$ *versus* 100%; Fig. 7*B*). This result demonstrated that the increased α3 subunit protein expression is unrelated to mRNA abundance and is consistent with a similar finding in the cerebellum of homozygous α1 subunit deletion mice (17).

Het$_{\alpha1}$KO Did Not Recruit α1 Subunit-containing GABA$_A$R from the Endoplasmic Reticulum—It was possible that Het$_{\alpha1}$KO increased the relative surface α1 subunit expression by recruiting α1 subunit-containing receptors from the ER. A substantial proportion of recombinant GABA$_A$Rs expressed in both heterologous cells and neurons is localized within the ER (32, 54). We determined the effect of Het$_{\alpha1}$KO on the fraction of ER-resident α1 subunits by measuring the proportion of subunit that contained high mannose, *N*-linked glycosylation, a marker of an ER-associated protein (55–57). Digestion with endo-H removes high mannose ER-associated, *N*-linked carbohydrates, whereas digestion with PNGase F removes all *N*-linked carbohydrates. We digested protein lysates from COS-7 cells transfected with α1β2γ2 receptors (positive control) and from wild type and Het$_{\alpha1}$KO cortices with endo-H or PNGase F and analyzed the digestion products by Western blot (Fig. 8). As described previously (32), PNGase F digestion of α1

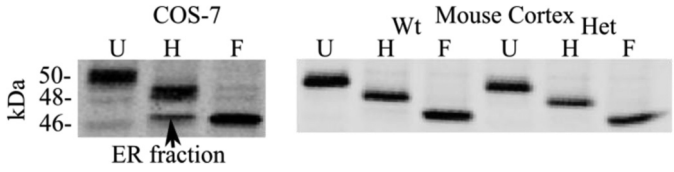

FIGURE 8. **Het$_{\alpha1}$KO did not alter the fraction α1 subunits associated with the ER.** We transfected COS-7 cells with $\alpha1\beta2\gamma2$ cDNA (positive control) and prepared homogenates from the COS-7 cells as well as from cortices of wild type and Het$_{\alpha1}$KO (*Het*) mice. We left the protein homogenates undigested (*U*), or digested them with either endo-H (*H*) or PNGase F (*F*). We analyzed the digestion products by Western blot and stained for the α1 subunit. In both COS-7 cells and cortical lysates, PNGase F digestion reduced the molecular mass of α1 subunit from 50 to 46 kDa, consistent with the removal of two glycans. Endo-H digestion of α1 subunit expressed in COS-7 cells produced a 46-kDa digestion product (ER fraction) and a 48-kDa product. Endo-H digestion of α1 subunit from wild type or Het$_{\alpha1}$KO cortex produced only the 48-kDa product ($n = 5$).

subunit reduced its apparent mass from 50 to 46 kDa, a finding consistent with the removal of its two *N*-linked glycans, and endo-H digestion of recombinant α1 subunits produced two products with different molecular masses, 46 kDa (ER-associated) and 48 kDa (not ER-associated). However, in wild type and Het$_{\alpha1}$KO cortices, endo-H digestion produced only a 48-kDa product (not ER-associated; $n = 5$). Therefore, in both wild type and Het$_{\alpha1}$KO mice, no substantial α1 subunit is present within the ER, and thus Het$_{\alpha1}$KO cannot increase the relative surface expression of the α1 subunit by recruiting ER-resident α1 subunit-containing GABA$_A$R to the cell surface.

Het$_{\alpha1}$KO Altered GABA$_A$R Endocytosis/Recycling—Previous studies demonstrated that modulation of dynamin-mediated endocytosis of GABA$_A$Rs regulates their surface expression (58–61). Patch clamp electrophysiological recordings that measured time-dependent changes in current amplitudes following the application of inhibitors of dynamin-mediated endocytosis have been used to study neurotransmitter receptor endocytosis in multiple regions in intact brain slices (29, 34–38). Although biochemical or immunohistochemical confirmation of increased neurotransmitter receptor surface expression after endocytosis inhibition has not typically been performed in intact brain slices, it has been confirmed in numerous studies of cultured cells (62–64) as well as in one study of hippocampal brain slices (29). Therefore, it is thought that increased current amplitude after endocytosis inhibition reflects increased surface expression of the neurotransmitter receptor. Here, we evaluated the effects of two inhibitors of dynamin-mediated endocytosis on GABAergic currents in layer VI somatosensory cortical neurons to determine whether Het$_{\alpha1}$KO altered endocytosis.

We first determined the effects of dynasore, a membrane-permeable inhibitor of dynamin's GTPase activity. We recorded base-line mIPSCs for 5 min and then added 80 μM dynasore and recorded mIPSCs for an additional 20 min. Inhibition of endocytosis caused time-dependent increases in mIPSC peak amplitudes in wild type ($n = 5$) but not Het$_{\alpha1}$KO ($n = 6$) neurons (Fig. 9, *A* and *B*). In wild type neurons, mIPSC peak amplitudes 20 min after dynasore administration were 126 ± 9.4% those of base-line recordings, but in Het$_{\alpha1}$KO neurons, peak amplitudes were only 87 ± 7.9% those of the baseline ($p = 0.014$, wild type compared with Het$_{\alpha1}$KO; $p = 0.101$, Het$_{\alpha1}$KO *versus* 100%). Dynasore did not significantly change

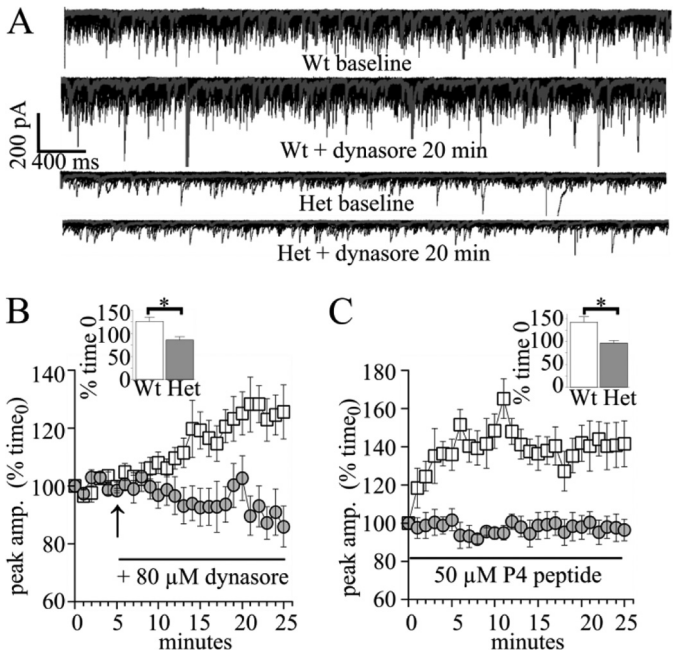

FIGURE 9. **Inhibition of dynamin-mediated endocytosis increased wild type, but not Het$_{\alpha1}$KO mIPSC amplitudes.** We tested the effects of 80 μM dynasore (*A* and *B*) and 50 μM P4 peptide (*C*), two inhibitors of dynamin-mediated endocytosis, on mIPSCs from wild type and Het$_{\alpha1}$KO layer VI pyramidal neurons. For dynasore, we recorded for a 5-min base-line period before adding the dynasore to the external recording solution. P4 peptide experiments were performed with P4 peptide in the internal solution of the patch pipette. Both recordings lasted 25 min. For both dynasore and P4 peptide, we averaged the mIPSC amplitudes in 1-min blocks and normalized them to the average amplitude during the first minute of recording (*baseline*). *A*, representative mIPSCs during the base line and 20 min after the addition of dynasore. We plotted the base line-normalized mIPSC amplitudes in *B* and *C* and compared the effects of the drugs at 25 min of recording (*insets*). Both dynasore ($n \geq 5$) and P4 peptide ($n = 5$) increased mIPSC peak amplitudes in wild type (□, *white*), but not Het$_{\alpha1}$KO (○, *gray*; $n = 6$) neurons. For dynasore, wild type mIPSC peak amplitudes were 126 ± 9.4% at 25 min compared with base line, but for Het$_{\alpha1}$KO neurons, amplitudes at 25 min were 87 ± 7.9% that of base line ($p = 0.014$). For P4 peptide, wild type mIPSC peak amplitudes were 142 ± 12% at 25 min compared with base line, but Het$_{\alpha1}$KO amplitudes at 25 min were 96 ± 5.5% compared with base line ($p = 0.009$). *Error bars*, S.E.

the time constant of current decay for either wild type ($p = 0.340$) or Het$_{\alpha1}$KO neurons ($p = 0.669$).

Next, we tested the effects of P4 peptide, a membrane-impermeable peptide that blocks the binding of dynamin with amphiphysin. We added P4 peptide to the internal solution of the patch pipette and recorded mIPSCs (Fig. 9*C*). In concordance with the dynasore results, the intracellular administration of P4 peptide caused time-dependent increases in mIPSC amplitudes in wild type but not Het$_{\alpha1}$KO neurons. After 25 min of recording with P4 peptide, mIPSC amplitudes from wild type neurons were 142 ± 12% the amplitude of those at the beginning of the recording, whereas mIPSC amplitudes from Het$_{\alpha1}$KO neurons were 96 ± 6% of base line ($n = 5$, $p = 0.009$). P4 peptide did not significantly change the time constant of current decay for either wild type ($p = 0.208$) or Het$_{\alpha1}$KO neurons ($p = 0.582$).

The observation that dynasore and P4 peptide caused time-dependent increases of mIPSC amplitudes in wild type but not Het$_{\alpha1}$KO neurons is consistent with endocytosis inhibition increasing the surface expression of GABA$_A$Rs in wild type neurons. Although, conceivably, dynasore and P4 peptide could

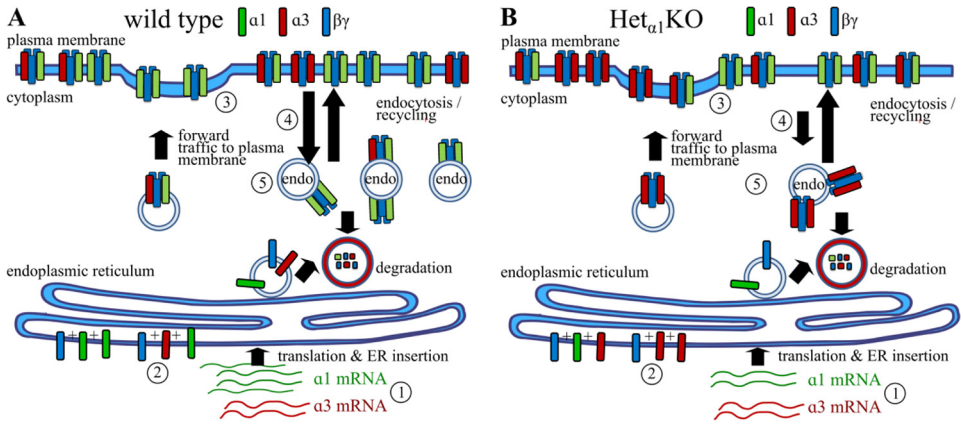

FIGURE 10. **The effects of Het$_{α1}$KO on cortical GABA$_A$R expression, composition, and endocytosis.** Here, we summarize our findings and propose a model by which Het$_{α1}$KO alters GABA$_A$R expression, composition, and endocytosis. For wild type (*A*) and Het$_{α1}$KO (*B*) neurons, we depict the plasma membrane (*top*), cytosol (*middle*), endoplasmic reticulum (*bottom*), α1 subunits (*green*), and α3 subunits (*red*). For simplicity, we grouped the partnering β and γ subunits as a *single blue symbol*, did not differentiate between lysosomal or proteosomal degradation, and did not depict the Golgi. *1*, Het$_{α1}$KO reduces functional α1 subunit mRNA but does not affect α3 subunit mRNA. *2*, therefore, Het$_{α1}$KO reduces α1 subunit translated and inserted into ER, and thus a greater fraction of α1 subunits assemble into hybrid α1α3βγ pentamers and a greater fraction of α3 subunits incorporate into α3βγ pentamers. Because fewer α1 subunits are able to compete with α3 subunits for binding partners, more α3 subunits incorporate into functional receptors and fewer undergo ER-associated degradation. Consistent with our glycosylation experiments, the ER does not contain a substantial pool of GABA$_A$R. *3*, there is a small reduction in total and surface GABA$_A$R. In addition, although the total number of α1 subunits is reduced, redistribution of GABA$_A$R from the cytoplasm increases the ratio of surface/total α1 subunits with a greater fraction in α1α3βγ pentamers. *4*, reduced cell surface endocytosis increases relative surface GABA$_A$R expression and decreases GABA$_A$R in early endosomes, an effect that reduces insertion into plasma membrane when endocytosis is inhibited with dynasore or P4 peptide (*5*).

indirectly increase peak current amplitudes of wild type neurons by preventing endocytosis of another protein that positively modulates GABA$_A$R function, our finding that neither dynasore nor P4 peptide altered the time course of mIPSC decay supports our interpretation that currents are enhanced due to increased receptor surface expression and not by alteration of receptor physiology.

The lack of effect of endocytosis inhibition on Het$_{α1}$KO currents, coupled with the observations that Het$_{α1}$KO increased the relative surface expression of the α1 subunit (Fig. 2) and α3 subunit expression (Fig. 3), suggests that Het$_{α1}$KO decreased the rate of base-line GABA$_A$R endocytosis and thereby reduced the amount GABA$_A$R in early endosomes available to recycle to the plasma membrane.

DISCUSSION

It is critical to characterize the molecular mechanisms that modulate inhibitory neurotransmission in epilepsy syndromes in order to elucidate the pathogenic mechanisms of these diseases. The Het$_{α1}$KO mouse is an excellent model of absence epilepsy that approximates the α1(S326fs328X) mutation associated with human absence epilepsy and possesses electrographic and behavioral absence seizures that respond to ethosuximide, a prototypical anti-absence epilepsy drug (13). Here, we found that Het$_{α1}$KO changed the total and surface expression and composition of synaptic-type GABA$_A$Rs and altered the physiology and pharmacology of synaptic inhibitory currents. In addition, we determined that Het$_{α1}$KO altered GABA$_A$R endocytosis/recycling and thus identified a biochemical mechanism that alters GABA$_A$R expression and may also contribute to the paroxysmal development of seizures.

Het$_{α1}$KO Alters Cortical GABA$_A$R Expression, Composition, and Physiology—Het$_{α1}$KO caused a small reduction in total and surface β2 subunit expression without affecting β3 subunit expression, results consistent with a modest reduction in GABA$_A$R number. In addition, Het$_{α1}$KO elicited three important effects on cortical total and surface α subunit expression (Fig 10). First, Het$_{α1}$KO increased the relative surface expression of the α1 subunit by causing significantly smaller reductions in surface than in total α1 subunit expression. Interestingly, another absence epilepsy-associated GABA$_A$R mutation, γ2(R43Q), reduced surface, but not total, γ2 subunit expression and did not alter total or surface α1 subunit expression (65). The apparent consistency of surface α1 subunit expression despite heterozygous α1 subunit deletion or γ2(R43Q) expression implies selectivity in GABA$_A$R isoform compensation, a finding that may be important for the study of both GABA$_A$R trafficking and epilepsy-associated disinhibition.

Second, Het$_{α1}$KO increased the total and surface expression of the α3 subunit. Previous Western blots and immunohistochemistry studies in Het$_{α1}$KO mice reached different conclusions concerning the effects of Het$_{α1}$KO on total α3 subunit expression (14, 21). Using both immunofluorescence as well as semiquantitative Western blots with linear protein detection, we demonstrated that Het$_{α1}$KO did increase total cortical α3 subunit expression. Importantly, we also showed that Het$_{α1}$KO substantially increased surface α3 subunit expression and thus the increased α3 subunit incorporated into cell surface receptors that could affect GABAergic physiology. In addition, our finding that Het$_{α1}$KO differentially reduced β2 but not β3 subunit expression raised the intriguing idea that α3 subunits may preferentially assemble with β3 rather than β2 subunits, a possibility consistent with observations that brain regions that selectively express the α3 subunit (*e.g.* reticular nucleus of the thalamus) express β3 but not β2 subunits (66).

Third, Het$_{α1}$KO increased the fraction of α1 subunits associated with α3 subunits and decreased the fraction of α3 subunits associated with α1 subunits. Conceivably, the association of α1 and α3 subunits could result from α1 and α3 subunits

associating in non-pentameric oligomers or in two separate but associated pentamers (*e.g.* connected by a scaffolding protein). However, previous gradient fractionation studies failed to detect non-pentameric assembly intermediates or substantial multipentameric complexes (67, 68), whereas the existence of "hybrid" GABA$_A$Rs containing two different α subunits has been well established (45). Therefore, it is likely that Het$_{\alpha1}$KO reduced the fraction of $\alpha1$ subunit in $\alpha1\beta\gamma$ receptors and increased the fraction of $\alpha1$ subunit in $\alpha1\alpha3\beta\gamma$ GABA$_A$Rs. In addition, it also decreased the fraction of $\alpha3$ subunits in $\alpha1\alpha3\beta\gamma$ receptors and increased the fraction in $\alpha3\beta\gamma$ GABA$_A$Rs (Fig. 10).

The increased mIPSC rise times, decay time constants, and reduced zolpidem responsiveness are consistent with the increase in surface $\alpha3$ subunit-containing GABA$_A$Rs. The reduction of Het$_{\alpha1}$KO in peak mIPSC amplitudes is undoubtedly partly related to the modest reduction in total GABA$_A$R number. However, because GABA$_A$Rs that contain $\alpha3$ subunits are less sensitive to GABA (larger EC$_{50}$) than $\alpha1$ subunit-containing GABA$_A$Rs (7, 69), the reduction in mIPSC peak current amplitude is also probably related to the partial substitution of $\alpha1$ subunit-containing GABA$_A$R with $\alpha3$ subunit-containing GABA$_A$R. This interpretation is supported by our observation that diazepam had a greater effect on Het$_{\alpha1}$KO than wild type eIPSCs. Diazepam acts, in part, by reducing the EC$_{50}$ of receptors for GABA (69). Therefore, the greater effect of diazepam on Het$_{\alpha1}$KO than on wild type neurons suggests that Het$_{\alpha1}$KO neurons have a higher GABA EC$_{50}$, consistent with increased expression of $\alpha3$ subunit-containing GABA$_A$Rs.

Because Het$_{\alpha1}$KO only modestly reduced surface $\alpha1$ subunit expression, it was somewhat unexpected that Het$_{\alpha1}$KO caused such substantial changes in GABA$_A$R physiology and pharmacology. However, this finding could be explained by our observation that Het$_{\alpha1}$KO increased the fraction of $\alpha1$ subunits assembling into hybrid $\alpha1\alpha3\beta\gamma$ receptors. Previous studies using recombinant concatenated subunits to force assembly of hybrid $\alpha1\alpha6\beta\gamma$ receptors demonstrated that the replacement of a single $\alpha1$ subunit in a pentamer substantially changed the pharmacology and physiology (46); a similar effect may be obtained by substituting an $\alpha3$ subunit for an $\alpha1$ subunit.

Het$_{\alpha1}$KO Alters GABA$_A$R Expression, in Part, by Reducing Base-line Endocytosis—Previous studies of GABA$_A$R subunits recombinantly overexpressed in neurons or heterologous cells demonstrated that GABA$_A$R pentamers formed rapidly in the ER but trafficked slowly to the cell surface and that a substantial pool of GABA$_A$Rs resided within the ER (70). We anticipated that the increased relative surface expression of the $\alpha1$ subunit in Het$_{\alpha1}$KO cortex could result from ER-resident GABA$_A$Rs recruited to the cell surface. Interestingly, in both wild type and Het$_{\alpha1}$KO cortex, no ER-associated $\alpha1$ subunit could be detected. It is likely that with native expression, in contrast to overexpression, reduced α subunit translation limits the amount of ER-associated protein.

Although Het$_{\alpha1}$KO did not recruit ER-associated $\alpha1$ subunits to the surface, it could still indirectly increase GABA$_A$R forward trafficking. Because GABA$_A$R pentamers assemble in the ER, our observation that Het$_{\alpha1}$KO altered $\alpha1$ and $\alpha3$ subunit association demonstrated that Het$_{\alpha1}$KO modified an ER-associated process. Possibly, the reduced expression of $\alpha1$ subunit allowed more $\alpha3$ subunits to assemble into functional receptors, which reduced $\alpha3$ subunit destruction via ER-associated degradation and thus indirectly enhanced trafficking of $\alpha3$ subunit-containing GABA$_A$R.

Het$_{\alpha1}$KO altered the response of neurons to dynasore and P4 peptide. Because Het$_{\alpha1}$KO increased and did not decrease the relative surface expression of the $\alpha1$ subunit and increased the expression of $\alpha3$ subunit-containing GABA$_A$R, it is unlikely that this finding resulted from Het$_{\alpha1}$KO directly decreasing the rates of GABA$_A$Rs trafficking from the Golgi or recycling after endocytosis. More likely, Het$_{\alpha1}$KO decreased the rate of base-line GABA$_A$R endocytosis and thus reduced the amount of GABA$_A$R in early endosomes capable of recycling GABA$_A$R to the membrane (Fig 10). The reduction of base-line GABA$_A$R endocytosis in Het$_{\alpha1}$KO cortices would increase $\alpha3$ subunit expression as well as the relative surface expression of the $\alpha1$ subunit.

It has been shown that modulating the rate of GABA$_A$R endocytosis dynamically controls synaptic GABA$_A$R expression. Phosphorylation of both the $\beta3$ and $\gamma2$ subunits decreases the interaction of the clathrin adapter protein, AP2, with the GABA$_A$R and thereby reduces endocytosis (60, 61, 71), whereas protein kinase C, acting through the $\beta2$ subunit, enhances endocytosis (72). Possibly, Het$_{\alpha1}$KO alters phosphorylation, which diminishes endocytosis and thereby reduces GABA$_A$R in early endosomes and increases the surface expression of the $\alpha3$ and $\alpha1$ subunit-containing GABA$_A$R.

The Effects of Het$_{\alpha1}$KO on GABA$_A$R Composition, Physiology, and Endocytosis May Predispose the Cortex to Initiate Seizures—Neurophysiological studies have demonstrated that humans and rodents with absence epilepsy possess hyperexcitable cortices (3–5). Here, we demonstrated that Het$_{\alpha1}$KO absence epilepsy mice exhibited altered cortical GABA$_A$R expression and composition, reduced peak current amplitudes, and increased decay times in layer VI pyramidal neurons, the layer thought to initiate absence seizures (40). The reduced GABAergic current amplitudes would disinhibit these layer VI neurons, rendering them more likely to initiate a seizure. Although reduced synaptic GABAergic currents have been reported in upper cortical layers for other rodent models of absence epilepsy (65, 73), to our knowledge, this is the first report demonstrating GABAergic synaptic dysfunction in the critical cortical layer VI.

Prolonged IPSC decay times have not been reported in previous studies of absence epilepsy. Possibly, increased decay times partially compensate for the reduced peak current amplitudes by partly normalizing the charge transfer of chloride ions. However, it is also possible that the prolonged decay times exacerbate seizures by promoting neuronal synchrony or enhancing the deinactivation of T-type calcium channels (74). Pharmacological or genetic interventions that selectively reduce IPSC decay will help elucidate the possible compensatory and exacerbating effects of prolonged IPSC decay on absence seizures.

The effects of Het$_{\alpha1}$KO on endocytosis/recycling may also be related to the seizures. Previous studies demonstrated that pharmacologically induced high frequency neuronal activity decreased GABA$_A$R endocytosis and thereby increased

$GABA_AR$ surface expression (1). Thus, it is possible that the absence seizures altered $GABA_AR$ endocytosis/recycling. In addition, it is clear from Fig. 9 that the alteration of endocytosis/recycling has been maximized; neither dynasore nor P4 peptide elicited any increase in mIPSC amplitudes in $Het_{\alpha1}KO$ cortices. This inability to dynamically increase GABAergic transmission could explain why seizures occur paroxysmally; neurons are incapable of mobilizing a reserve of cytoplasmic $GABA_ARs$ in response to periods of high frequency neuronal activity. Future studies that specifically examine the effects of absence seizures on $GABA_AR$ endocytosis will help to determine if the seizures elicit this compensatory response or if the lack of a rapidly accessible reserve of $GABA_AR$ leaves neurons vulnerable to periodic stresses, prompting them to initiate absence seizures.

Acknowledgments—We gratefully acknowledge Drs. Andre Lagrange, Aurelio Galli, and Robert Macdonald (Vanderbilt University) for helpful comments and suggestions.

REFERENCES

1. Rannals, M. D., and Kapur, J. (2011) Homeostatic strengthening of inhibitory synapses is mediated by the accumulation of $GABA_A$ receptors. *J. Neurosci.* **31,** 17701–17712
2. Shu, Y., Hasenstaub, A., and McCormick, D. A. (2003) Turning on and off recurrent balanced cortical activity. *Nature* **423,** 288–293
3. Lüttjohann, A., Zhang, S., de Peijper, R., and van Lijtelaar, G. (2011) Electrical stimulation of the epileptic focus in absence epileptic WAG/Rij rats. Assessment of local and network excitability. *Neuroscience* **188,** 125–134
4. Badawy, R. A., and Jackson, G. D. (2012) Cortical excitability in migraine and epilepsy. A common feature? *J. Clin. Neurophysiol.* **29,** 244–249
5. Fedi, M., Berkovic, S. F., Macdonell, R. A., Curatolo, J. M., Marini, C., and Reutens, D. C. (2008) Intracortical hyperexcitability in humans with a $GABA_A$ receptor mutation. *Cereb. Cortex* **18,** 664–669
6. Sieghart, W. (2006) Structure, pharmacology, and function of $GABA_A$ receptor subtypes. *Adv. Pharmacol.* **54,** 231–263
7. Picton, A. J., and Fisher, J. L. (2007) Effect of the α subunit subtype on the macroscopic kinetic properties of recombinant $GABA_A$ receptors. *Brain Res.* **1165,** 40–49
8. Cossette, P., Liu, L., Brisebois, K., Dong, H., Lortie, A., Vanasse, M., Saint-Hilaire, J. M., Carmant, L., Verner, A., Lu, W. Y., Wang, Y. T., and Rouleau, G. A. (2002) Mutation of GABRA1 in an autosomal dominant form of juvenile myoclonic epilepsy. *Nat. Genet.* **31,** 184–189
9. Lachance-Touchette, P., Brown, P., Meloche, C., Kinirons, P., Lapointe, L., Lacasse, H., Lortie, A., Carmant, L., Bedford, F., Bowie, D., and Cossette, P. (2011) Novel $\alpha1$ and $\gamma2$ $GABA_A$ receptor subunit mutations in families with idiopathic generalized epilepsy. *Eur. J Neurosci.* **34,** 237–249
10. Maljevic, S., Krampfl, K., Cobilanschi, J., Tilgen, N., Beyer, S., Weber, Y. G., Schlesinger, F., Ursu, D., Melzer, W., Cossette, P., Bufler, J., Lerche, H., and Heils, A. (2006) A mutation in the $GABA_A$ receptor α_1-subunit is associated with absence epilepsy. *Ann. Neurol.* **59,** 983–987
11. Ding, L., Feng, H. J., Macdonald, R. L., Botzolakis, E. J., Hu, N., and Gallagher, M. J. (2010) The $GABA_A$ receptor $\alpha1$ subunit mutation A322D associated with autosomal dominant juvenile myoclonic epilepsy reduces the expression and alters the composition of wild type $GABA_A$ receptors. *J. Biol. Chem.* **285,** 26390–26405
12. Kang, J. Q., Shen, W., and Macdonald, R. L. (2009) Two molecular pathways (NMD and ERAD) contribute to a genetic epilepsy associated with the $GABA_A$ receptor GABRA1 PTC mutation, 975delC, S326fs328X. *J. Neurosci.* **29,** 2833–2844
13. Arain, F. M., Boyd, K. L., and Gallagher, M. J. (2012) Decreased viability and absence-like epilepsy in mice lacking or deficient in the $GABA_A$ receptor $\alpha1$ subunit. *Epilepsia* **53,** e161–e165
14. Kralic, J. E., Korpi, E. R., O'Buckley, T. K., Homanics, G. E., and Morrow, A. L. (2002) Molecular and pharmacological characterization of $GABA_A$ receptor $\alpha1$ subunit knockout mice. *J. Pharmacol. Exp. Ther.* **302,** 1037–1045
15. Kralic, J. E., Sidler, C., Parpan, F., Homanics, G. E., Morrow, A. L., and Fritschy, J. M. (2006) Compensatory alteration of inhibitory synaptic circuits in cerebellum and thalamus of γ-aminobutyric acid type A receptor $\alpha1$ subunit knockout mice. *J. Comp. Neurol.* **495,** 408–421
16. Lagier, S., Panzanelli, P., Russo, R. E., Nissant, A., Bathellier, B., Sassoè-Pognetto, M., Fritschy, J. M., and Lledo, P. M. (2007) GABAergic inhibition at dendrodendritic synapses tunes γ oscillations in the olfactory bulb. *Proc. Natl. Acad. Sci. U.S.A.* **104,** 7259–7264
17. Ogris, W., Lehner, R., Fuchs, K., Furtmüller, B., Höger, H., Homanics, G. E., and Sieghart, W. (2006) Investigation of the abundance and subunit composition of $GABA_A$ receptor subtypes in the cerebellum of $\alpha1$-subunit-deficient mice. *J. Neurochem.* **96,** 136–147
18. Peden, D. R., Petitjean, C. M., Herd, M. B., Durakoglugil, M. S., Rosahl, T. W., Wafford, K., Homanics, G. E., Belelli, D., Fritschy, J. M., and Lambert, J. J. (2008) Developmental maturation of synaptic and extrasynaptic $GABA_A$ receptors in mouse thalamic ventrobasal neurones. *J. Physiol.* **586,** 965–987
19. Schneider Gasser, E. M., Duveau, V., Prenosil, G. A., and Fritschy, J. M. (2007) Reorganization of GABAergic circuits maintains $GABA_A$ receptor-mediated transmission onto CA1 interneurons in $\alpha1$-subunit-null mice. *Eur. J. Neurosci.* **25,** 3287–3304
20. Sur, C., Wafford, K. A., Reynolds, D. S., Hadingham, K. L., Bromidge, F., Macaulay, A., Collinson, N., O'Meara, G., Howell, O., Newman, R., Myers, J., Atack, J. R., Dawson, G. R., McKernan, R. M., Whiting, P. J., and Rosahl, T. W. (2001) Loss of the major $GABA_A$ receptor subtype in the brain is not lethal in mice. *J. Neurosci.* **21,** 3409–3418
21. Zeller, A., Crestani, F., Camenisch, I., Iwasato, T., Itohara, S., Fritschy, J. M., and Rudolph, U. (2008) Cortical glutamatergic neurons mediate the motor sedative action of diazepam. *Mol. Pharmacol.* **73,** 282–291
22. Vicini, S., Ferguson, C., Prybylowski, K., Kralic, J., Morrow, A. L., and Homanics, G. E. (2001) $GABA_A$ receptor $\alpha1$ subunit deletion prevents developmental changes of inhibitory synaptic currents in cerebellar neurons. *J. Neurosci.* **21,** 3009–3016
23. Yee, B. K., Keist, R., von Boehmer, L., Studer, R., Benke, D., Hagenbuch, N., Dong, Y., Malenka, R. C., Fritschy, J. M., Bluethmann, H., Feldon, J., Möhler, H., and Rudolph, U. (2005) A schizophrenia-related sensorimotor deficit links $\alpha3$-containing $GABA_A$ receptors to a dopamine hyperfunction. *Proc. Natl. Acad. Sci. U.S.A.* **102,** 17154–17159
24. Schofield, C. M., Kleiman-Weiner, M., Rudolph, U., and Huguenard, J. R. (2009) A gain in $GABA_A$ receptor synaptic strength in thalamus reduces oscillatory activity and absence seizures. *Proc. Natl. Acad. Sci. U.S.A.* **106,** 7630–7635
25. Zhou, C., Lippman, J. J., Sun, H., and Jensen, F. E. (2011) Hypoxia-induced neonatal seizures diminish silent synapses and long-term potentiation in hippocampal CA1 neurons. *J. Neurosci.* **31,** 18211–18222
26. Moyer, J. R., Jr., and Brown, T. H. (1998) Methods for whole-cell recording from visually preselected neurons of perirhinal cortex in brain slices from young and aging rats. *J. Neurosci. Methods* **86,** 35–54
27. Goodkin, H. P., Joshi, S., Mtchedlishvili, Z., Brar, J., and Kapur, J. (2008) Subunit-specific trafficking of $GABA_A$ receptors during status epilepticus. *J. Neurosci.* **28,** 2527–2538
28. Robertson, S. D., Matthies, H. J., Owens, W. A., Sathananthan, V., Christianson, N. S., Kennedy, J. P., Lindsley, C. W., Daws, L. C., and Galli, A. (2010) Insulin reveals Akt signaling as a novel regulator of norepinephrine transporter trafficking and norepinephrine homeostasis. *J. Neurosci.* **30,** 11305–11316
29. Terunuma, M., Xu, J., Vithlani, M., Sieghart, W., Kittler, J., Pangalos, M., Haydon, P. G., Coulter, D. A., and Moss, S. J. (2008) Deficits in phosphorylation of $GABA_A$ receptors by intimately associated protein kinase C activity underlie compromised synaptic inhibition during status epilepticus. *J. Neurosci.* **28,** 376–384
30. Puzzolo, E., and Mallamaci, A. (2010) Cortico-cerebral histogenesis in the opossum *Monodelphis domestica*. Generation of a hexalaminar neocortex in the absence of a basal proliferative compartment. *Neural Dev.* **5,** 8
31. Zhang, S. J., Buchthal, B., Lau, D., Hayer, S., Dick, O., Schwaninger, M., Veltkamp, R., Zou, M., Weiss, U., and Bading, H. (2011) A signaling cas-

cade of nuclear calcium-CREB-ATF3 activated by synaptic NMDA receptors defines a gene repression module that protects against extrasynaptic NMDA receptor-induced neuronal cell death and ischemic brain damage. *J. Neurosci.* **31,** 4978–4990
32. Gallagher, M. J., Shen, W., Song, L., and Macdonald, R. L. (2005) Endoplasmic reticulum retention and associated degradation of a GABA$_A$ receptor epilepsy mutation that inserts an aspartate in the M3 transmembrane segment of the α1 subunit. *J. Biol. Chem.* **280,** 37995–38004
33. Gallagher, M. J., Ding, L., Maheshwari, A., and Macdonald, R. L. (2007) The GABA$_A$ receptor α1 subunit epilepsy mutation A322D inhibits transmembrane helix formation and causes proteasomal degradation. *Proc. Natl. Acad. Sci. U.S.A.* **104,** 12999–13004
34. Kotowski, S. J., Hopf, F. W., Seif, T., Bonci, A., and von Zastrow, M. (2011) Endocytosis promotes rapid dopaminergic signaling. *Neuron* **71,** 278–290
35. Chen, G., Kittler, J. T., Moss, S. J., and Yan, Z. (2006) Dopamine D3 receptors regulate GABA$_A$ receptor function through a phospho-dependent endocytosis mechanism in nucleus accumbens. *J. Neurosci.* **26,** 2513–2521
36. Dennis, S. H., Jaafari, N., Cimarosti, H., Hanley, J. G., Henley, J. M., and Mellor, J. R. (2011) Oxygen/glucose deprivation induces a reduction in synaptic AMPA receptors on hippocampal CA3 neurons mediated by mGluR1 and adenosine A3 receptors. *J. Neurosci.* **31,** 11941–11952
37. Grueter, B. A., McElligott, Z. A., Robison, A. J., Mathews, G. C., and Winder, D. G. (2008) *In vivo* metabotropic glutamate receptor 5 (mGluR5) antagonism prevents cocaine-induced disruption of postsynaptically maintained mGluR5-dependent long-term depression. *J. Neurosci.* **28,** 9261–9270
38. Liu, W., Yuen, E. Y., Allen, P. B., Feng, J., Greengard, P., and Yan, Z. (2006) Adrenergic modulation of NMDA receptors in prefrontal cortex is differentially regulated by RGS proteins and spinophilin. *Proc. Natl. Acad. Sci. U.S.A.* **103,** 18338–18343
39. Meeren, H. K., Pijn, J. P., Van Luijtelaar, E. L., Coenen, A. M., and Lopes da Silva, F. H. (2002) Cortical focus drives widespread corticothalamic networks during spontaneous absence seizures in rats. *J. Neurosci.* **22,** 1480–1495
40. Polack, P. O., Guillemain, I., Hu, E., Deransart, C., Depaulis, A., and Charpier, S. (2007) Deep layer somatosensory cortical neurons initiate spike-and-wave discharges in a genetic model of absence seizures. *J. Neurosci.* **27,** 6590–6599
41. Rudy, B., Fishell, G., Lee, S., and Hjerling-Leffler, J. (2011) Three groups of interneurons account for nearly 100% of neocortical GABAergic neurons. *Dev. Neurobiol.* **71,** 45–61
42. Heller, E. A., Zhang, W., Selimi, F., Earnheart, J. C., Ślimak, M. A., Santos-Torres, J., Ibañez-Tallon, I., Aoki, C., Chait, B. T., and Heintz, N. (2012) The biochemical anatomy of cortical inhibitory synapses. *PLoS ONE* **7,** e39572
43. Hutcheon, B., Fritschy, J. M., and Poulter, M. O. (2004) Organization of GABA receptor α-subunit clustering in the developing rat neocortex and hippocampus. *Eur. J. Neurosci.* **19,** 2475–2487
44. Yu, Z. Y., Wang, W., Fritschy, J. M., Witte, O. W., and Redecker, C. (2006) Changes in neocortical and hippocampal GABA$_A$ receptor subunit distribution during brain maturation and aging. *Brain Res.* **1099,** 73–81
45. Benke, D., Fakitsas, P., Roggenmoser, C., Michel, C., Rudolph, U., and Mohler, H. (2004) Analysis of the presence and abundance of GABA$_A$ receptors containing two different types of α subunits in murine brain using point-mutated α subunits. *J. Biol. Chem.* **279,** 43654–43660
46. Minier, F., and Sigel, E. (2004) Positioning of the α-subunit isoforms confers a functional signature to γ-aminobutyric acid type A receptors. *Proc. Natl. Acad. Sci. U.S.A.* **101,** 7769–7774
47. Barberis, A., Mozrzymas, J. W., Ortinski, P. I., and Vicini, S. (2007) Desensitization and binding properties determine distinct $\alpha1\beta2\gamma2$ and $\alpha3\beta2\gamma2$ GABA$_A$ receptor-channel kinetic behavior. *Eur. J Neurosci.* **25,** 2726–2740
48. Rula, E. Y., Lagrange, A. H., Jacobs, M. M., Hu, N., Macdonald, R. L., and Emeson, R. B. (2008) Developmental modulation of GABA$_A$ receptor function by RNA editing. *J. Neurosci.* **28,** 6196–6201
49. Jia, F., Goldstein, P. A., and Harrison, N. L. (2009) The modulation of synaptic GABA$_A$ receptors in the thalamus by eszopiclone and zolpidem. *J. Pharmacol. Exp. Ther.* **328,** 1000–1006
50. Kang-Park, M. H., Wilson, W. A., and Moore, S. D. (2004) Differential actions of diazepam and zolpidem in basolateral and central amygdala nuclei. *Neuropharmacology* **46,** 1–9
51. Petroski, R. E., Pomeroy, J. E., Das, R., Bowman, H., Yang, W., Chen, A. P., and Foster, A. C. (2006) Indiplon is a high-affinity positive allosteric modulator with selectivity for α1 subunit-containing GABA$_A$ receptors. *J. Pharmacol. Exp. Ther.* **317,** 369–377
52. Popik, P., Kostakis, E., Krawczyk, M., Nowak, G., Szewczyk, B., Krieter, P., Chen, Z., Russek, S. J., Gibbs, T. T., Farb, D. H., Skolnick, P., Lippa, A. S., and Basile, A. S. (2006) The anxioselective agent 7-(2-chloropyridin-4-yl)pyrazolo-[1,5-a]-pyrimidin-3-yl](pyridin-2-yl)methanone (DOV 51892) is more efficacious than diazepam at enhancing GABA-gated currents at α1 subunit-containing GABA$_A$ receptors. *J. Pharmacol. Exp. Ther.* **319,** 1244–1252
53. Paz, J. T., Bryant, A. S., Peng, K., Fenno, L., Yizhar, O., Frankel, W. N., Deisseroth, K., and Huguenard, J. R. (2011) A new mode of corticothalamic transmission revealed in the Gria4$^{-/-}$ model of absence epilepsy. *Nat. Neurosci.* **14,** 1167–1173
54. Saliba, R. S., Pangalos, M., and Moss, S. J. (2008) The ubiquitin-like protein Plic-1 enhances the membrane insertion of GABA$_A$ receptors by increasing their stability within the endoplasmic reticulum. *J. Biol. Chem.* **283,** 18538–18544
55. Bagley, D. C., Paradkar, P. N., Kaplan, J., and Ward, D. M. (2012) Mon1a protein acts in trafficking through the secretory apparatus. *J. Biol. Chem.* **287,** 25577–25588
56. Helenius, A., and Aebi, M. (2004) Roles of *N*-linked glycans in the endoplasmic reticulum. *Annu. Rev. Biochem.* **73,** 1019–1049
57. Lo, W. Y., Botzolakis, E. J., Tang, X., and Macdonald, R. L. (2008) A conserved Cys-loop receptor aspartate residue in the M3-M4 cytoplasmic loop is required for GABA$_A$ receptor assembly. *J. Biol. Chem.* **283,** 29740–29752
58. Kittler, J. T., Delmas, P., Jovanovic, J. N., Brown, D. A., Smart, T. G., and Moss, S. J. (2000) Constitutive endocytosis of GABA$_A$ receptors by an association with the adaptin AP2 complex modulates inhibitory synaptic currents in hippocampal neurons. *J. Neurosci.* **20,** 7972–7977
59. Kittler, J. T., Thomas, P., Tretter, V., Bogdanov, Y. D., Haucke, V., Smart, T. G., and Moss, S. J. (2004) Huntingtin-associated protein 1 regulates inhibitory synaptic transmission by modulating γ-aminobutyric acid type A receptor membrane trafficking. *Proc. Natl. Acad. Sci. U.S.A.* **101,** 12736–12741
60. Kittler, J. T., Chen, G., Honing, S., Bogdanov, Y., McAinsh, K., Arancibia-Carcamo, I. L., Jovanovic, J. N., Pangalos, M. N., Haucke, V., Yan, Z., and Moss, S. J. (2005) Phospho-dependent binding of the clathrin AP2 adaptor complex to GABA$_A$ receptors regulates the efficacy of inhibitory synaptic transmission. *Proc. Natl. Acad. Sci. U.S.A.* **102,** 14871–14876
61. Kittler, J. T., Chen, G., Kukhtina, V., Vahedi-Faridi, A., Gu, Z., Tretter, V., Smith, K. R., McAinsh, K., Arancibia-Carcamo, I. L., Saenger, W., Haucke, V., Yan, Z., and Moss, S. J. (2008) Regulation of synaptic inhibition by phospho-dependent binding of the AP2 complex to a YECL motif in the GABA$_A$ receptor γ2 subunit. *Proc. Natl. Acad. Sci. U.S.A.* **105,** 3616–3621
62. Bogdanov, Y., Michels, G., Armstrong-Gold, C., Haydon, P. G., Lindstrom, J., Pangalos, M., and Moss, S. J. (2006) Synaptic GABAA receptors are directly recruited from their extrasynaptic counterparts. *EMBO J.* **25,** 4381–4389
63. Kim, J., Jung, S. C., Clemens, A. M., Petralia, R. S., and Hoffman, D. A. (2007) Regulation of dendritic excitability by activity-dependent trafficking of the A-type K^+ channel subunit Kv4.2 in hippocampal neurons. *Neuron* **54,** 933–947
64. Varkevisser, R., Houtman, M. J., Waasdorp, M., Man, J. C., Heukers, R., Takanari, H., Tieland, R. G., van Bergen En Henegouwen, P. M., Vos, M. A., and van der Heyden, M. A. (2013) Inhibiting the clathrin-mediated endocytosis pathway rescues K(IR)2.1 downregulation by pentamidine. *Pflugers Arch.* **465,** 247–259
65. Tan, H. O., Reid, C. A., Single, F. N., Davies, P. J., Chiu, C., Murphy, S., Clarke, A. L., Dibbens, L., Krestel, H., Mulley, J. C., Jones, M. V., Seeburg, P. H., Sakmann, B., Berkovic, S. F., Sprengel, R., and Petrou, S. (2007) Reduced cortical inhibition in a mouse model of familial childhood absence epilepsy. *Proc. Natl. Acad. Sci. U.S.A.* **104,** 17536–17541

66. Eyre, M. D., Renzi, M., Farrant, M., and Nusser, Z. (2012) Setting the time course of inhibitory synaptic currents by mixing multiple GABA$_A$ receptor α subunit isoforms. *J. Neurosci.* **32,** 5853–5867
67. Klausberger, T., Ehya, N., Fuchs, K., Fuchs, T., Ebert, V., Sarto, I., and Sieghart, W. (2001) Detection and binding properties of GABA$_A$ receptor assembly intermediates. *J. Biol. Chem.* **276,** 16024–16032
68. Tretter, V., Ehya, N., Fuchs, K., and Sieghart, W. (1997) Stoichiometry and assembly of a recombinant GABA$_A$ receptor subtype. *J. Neurosci.* **17,** 2728–2737
69. Verdoorn, T. A. (1994) Formation of heteromeric γ-aminobutyric acid type A receptors containing two different α subunits. *Mol. Pharmacol.* **45,** 475–480
70. Gorrie, G. H., Vallis, Y., Stephenson, A., Whitfield, J., Browning, B., Smart, T. G., and Moss, S. J. (1997) Assembly of GABA$_A$ receptors composed of α1 and β2 subunits in both cultured neurons and fibroblasts. *J. Neurosci.* **17,** 6587–6596
71. Saliba, R. S., Kretschmannova, K., and Moss, S. J. (2012) Activity-dependent phosphorylation of GABA$_A$ receptors regulates receptor insertion and tonic current. *EMBO J.* **31,** 2937–2951
72. Herring, D., Huang, R., Singh, M., Dillon, G. H., and Leidenheimer, N. J. (2005) PKC modulation of GABA$_A$ receptor endocytosis and function is inhibited by mutation of a dileucine motif within the receptor β2 subunit. *Neuropharmacology* **48,** 181–194
73. Sasaki, S., Huda, K., Inoue, T., Miyata, M., and Imoto, K. (2006) Impaired feedforward inhibition of the thalamocortical projection in epileptic Ca^{2+} channel mutant mice, tottering. *J. Neurosci.* **26,** 3056–3065
74. Mann, E. O., and Mody, I. (2008) The multifaceted role of inhibition in epilepsy. Seizure-genesis through excessive GABAergic inhibition in autosomal dominant nocturnal frontal lobe epilepsy. *Curr. Opin. Neurol.* **21,** 155–160